

The Pennsylvania State University
The Graduate School
Department of Materials Science and Engineering

CONTACT ACTIVATION
OF BLOOD-PLASMA COAGULATION

A Thesis in
Materials Science and Engineering
by
Tanisha Diggs

© 2008 Tanisha Diggs

Submitted in Partial Fulfillment
of the Requirements
for the Degree of

Master of Science

August 2008

The thesis of Tanisha Diggs was reviewed and approved* by the following:

Erwin A. Vogler
Professor of Materials Science and
Engineering and Bioengineering
Thesis Advisor

Christopher A. Siedlecki
Associate Professor of Surgery
and Bioengineering

James P. Runt
Professor of Polymer Science

Joan M. Redwing
Professor of Materials Science and Engineering
Chair of the Intercollege Graduate Degree Program
in Materials Science and Engineering

* Signatures are on file in the Graduate School.

ABSTRACT

Initiation of the coagulation cascade ultimately leads to thrombus (clot) formation. This phenomenon impedes the production of hemocompatible biomaterials. Adverse reactions at the interface of a biomaterial in contact with the biological system, in this instance blood, start the contact activation mechanism. Upon initiation, blood-plasma coagulation proceeds through a sequence of zymogen-enzyme conversions; the complexity of this succession can quickly amplify into thrombus formation. Therefore, future innovation of cardiovascular biomaterials insists on additional information regarding blood-biomaterial interactions. In-vitro plasma coagulation assays, chromogenic assays and contact activation experiments establish dose-response relationships seeking to relate thrombogenicity to material properties. This thesis work utilizes these assays in attempt to better understand surface mediated bio-interactions. FXII is initially an inactive enzyme, also called a zymogen, activated in the contact activation mechanism by contact with a surface. The subsequent activation of FXIIa and/or FXIIc are two possible outcomes following contact activation. Results from this thesis proves contact activation yield at hydrophobic surfaces in neat FXII solution was greater than hydrophilic surfaces in neat FXII solution by plasma coagulation assay and by chromogenic assay. Additionally, this thesis provides evidence that FXIIc has procoagulant activity as well as amidolytic activity that can activate the intrinsic pathway. Prior research suggests autohydrolysis is a significant reaction in the FXIIa chromogenic assay. This thesis confirms the same results; however, results reported herein confirm that autohydrolysis is not a significant reaction in the FXIIc chromogenic assay. Additionally, plasma coagulation assays show that FXIIc is 2.6 times weaker procoagulant than FXIIa on a molar basis.

TABLE OF CONTENTS

LIST OF FIGURES	vi
LIST OF TABLES	viii
LIST OF EQUATIONS	ix
LIST OF ABBREVIATIONS	x
Chapter 1. INTRODUCTION	1
1.1 Background	1
1.2 Biomaterials, Biocompatibility and Surface Properties	1
1.3 Blood and Coagulation	5
1.4 Chromogenic Substrates	8
1.5 Objectives	9
Chapter 2. MATERIALS AND METHODS	10
2.1 Materials	10
2.1.1 General Materials.....	10
2.1.2 Platelet Poor Plasma (PPP)	11
2.1.3 Coagulation Proteins	11
2.1.4 Chromogenic Substrate	11
2.1.5 Procoagulant Surfaces	12
2.2 Methods	13
2.2.1 Plasma Coagulation Time Assay for FXIIa and FXIIIf	13
2.2.2 Chromogenic Assay for FXIIa and FXIIIf	14
2.2.3 Surface activation of FXII in neat-buffer solution	15
2.2.4 Statistical Analysis	16
Chapter 3. RESULTS	17
3.1 Plasma Coagulation Time Assay for FXIIa and FXIIIf	17
3.2 Contact angle measurements of procoagulant materials	21

3.3 FXIIa generation by surface activation of FXII in neat-buffer solution by plasma coagulation assay.....	22
3.4 Chromogenic Assay for FXIIa and FXIIf	26
3.5 FXIIa generation by surface activation of FXII in neat-buffer solution by chromogenic assay.....	30
 Chapter 4. DISCUSSION	 33
4.1 Plasma Coagulation Time Assay for FXIIa and FXIIf	33
4.2 FXIIa generation by surface activation of FXII in neat-buffer solution by plasma coagulation assay.....	33
4.3 Chromogenic Assay for FXIIa and FXIIf	34
4.4 FXIIa generation by surface activation of FXII in neat-buffer solution by chromogenic assay	35
 Chapter 5. CONCLUSIONS	 36
 BIBLIOGRAPHY	 38
APPENDIX A: Coagulation Cascade Components	41
APPENDIX B: Calculations.....	43

LIST OF FIGURES

Figure 1: Illustration of contact angles on hydrophilic and hydrophobic surfaces	4
Figure 2: The Coagulation Cascade illustrating the three different pathways: intrinsic, extrinsic and common pathway	6
Figure 3: Contact activation of blood coagulation	8
Figure 4: S-2302 Structure	12
Figure 5: Schematic illustration of the in-vitro coagulation assay depicting reagents and materials used, procedure and end result	14
Figure 6: Principle of chromogenic substrates and color formation.....	15
Figure 7: Experimental outline for detection of FXIIa produced by contact with procoagulant surfaces	16
Figure 8: FXIIa titration of PPP that relates observed plasma coagulation time to FXIIa concentration where n=5.....	17
Figure 9: FXIIa calibration curve obtained through exogenous FXIIa titration on log concentration axis where n=5.....	18
Figure 10: FXIIIf titration of PPP that relates observed plasma coagulation time to FXIIIf concentration where n=4.....	19
Figure 11: FXIIIf calibration curve obtained through exogenous FXIIIf titration on log concentration axis where n=4.....	20
Figure 12: Plot of Force (mN) vs. Immersion Depth (mm) of hydrophilic procoagulants using the wilhelmy method	21
Figure 13: Plot of Force (mN) vs. Immersion Depth (mm) of hydrophobic procoagulants using the wilhelmy method	22
Figure 14: FXIIa calibration curve obtained through exogenous FXIIa titration on log concentration axis	23
Figure 15: FXIIa generation in neat FXII solution at 30 $\mu\text{g}/\text{mL}$ induced by contact with 500 mm^2 surface area of hydrophobic and hydrophilic procoagulants	25
Figure 16: Color development kinetics for chromogenic FXIIa assay performed in neat-buffer solutions of FXII	26
Figure 17: Linear correlation between V_{max} and $[\text{FXIIa}]$	27

Figure 18: Linear correlation between V_{max} and [FXIIa]	28
Figure 19: Color development kinetics for chromogenic FXIIa assay performed in neat- buffer solutions of FXII	29
Figure 20: FXIIa calibration curve that relates absorbance rate ($\Delta A/min$) to FXIIa concentration obtained through exogenous FXIIa titration of chromogenic substrate	30
Figure 21: FXIIa generation in neat FXII solution at 30 $\mu g/mL$ induced by contact with 500 mm^2 surface area of hydrophobic and hydrophilic procoagulants	32

LIST OF TABLES

Table 1: Contact activation of FXII neat buffer solution induced by contact with hydrophilic (clean glass) and hydrophobic (silanized glass) producing FXIIa by plasma coagulation assay	24
Table 2: Contact activation of FXII neat buffer solution induced by contact with hydrophilic (clean glass) and hydrophobic (silanized glass) producing FXIIa by chromogenic assay	31

LIST OF EQUATIONS

Equation 1: Young Equation	4
----------------------------------	---

LIST OF ABBREVIATIONS AND SYMBOLS

CT	Coagulation Time
°C	Degrees Celsius
FXII	Human Coagulation Factor XII (Hageman Factor)
FXIIa	Human Coagulation Factor XIIa
FXIIa β /FXII β f	Human Coagulation Factor XIIa β /XII β f
γ_{lv}	Liquid-vapor Interfacial Tension
γ_{sl}	Solid-liquid Interfacial Tension
γ_{sv}	Solid-vapor Interfacial Tension
g	grams
kg	Kilograms
M	Molarity
m ³	cubic meters
mg	Milligrams
min.	minutes
mL	Milliliters
mm	Millimeters
M Ω	Megaohms
MW	Molecular Weight
n	Number
ng	Nanograms
OTS	Octadecyltrichlorosilane
PBS	Phosphate buffered saline
PEU	Plasma Equivalent Units
PPP	Human platelet poor plasma
r	radius
SA	surface area
sec.	seconds
τ	adhesion tension
Θ	Contact Angle

μg

Micrograms

μl

Microliters

μm

Micrometers

Chapter 1. INTRODUCTION

1.1 Background

Cardiovascular disease accounted for 36.3% of all deaths in the United States in year 2004. Nearly 80 million adults in the United States have one or more types of cardiovascular disease (CVD); some of which include coronary heart disease (CHD), peripheral arterial disease (PAD), carotid artery disease (CAD), stroke, heart failure (HF) and congenital cardiovascular defects. [1] Moreover, atherosclerotic cardiovascular disease is the number one cause of mortality in the western part of the world. [2] Atherosclerosis is the process in which plaque accumulates in the walls of different arteries throughout the body. Arteries sharply affected by this condition are the left and right main coronary arteries and their branches, the carotid artery, major branches of the abdominal aorta and the femoral and iliac arteries in the legs. [5] Peripheral artery disease, coronary artery disease and carotid artery disease are caused by the obstruction of the large peripheral arteries, coronary arteries and the carotid artery, respectively. Cardiovascular biomaterials and medical devices are exploited to improve these disease states, among many others. For instance, atherosclerosis can stop blood flow through the affected vessels requiring treatment by surgically bypassing the affected segment with a vascular graft to restore flow. [2]

The biological response to many of these existing devices are less than optimal. [3] Although millions of individuals have benefited from implanted biomaterials and disposable medical devices, the complexity of blood-material interactions can limit the lifetime of the implant. Engineering more hemocompatible materials requires a better understanding of the interaction between blood and a biomaterial surface.

1.2 Biomaterials, Biocompatibility and Surface Properties

Although biomaterials can be used for in-vitro applications, they are also integrated into devices or implants. [3] Biomaterials are defined as “non-viable material(s) used in medical device(s), intended to interact with biological systems” [4].

Some examples of these permanent or temporary in-vivo devices include catheters, stents, ventricular assist devices, vascular grafts, prosthetic heart valves, pacemaker leads and an artificial heart. Most biomaterial in-vitro applications are disposables that include blood collection tubes, tissue-culture dishes and plates, needles, syringes and other materials used for biomedical research. Biomaterials have had a major impact in the health care industry by saving and improving the quality of lives of humans. [5]

The interaction at the blood-biomaterial interface plays a major role in determining the biocompatibility of the specific application. Biocompatibility is defined as “the ability of a material to perform with an appropriate host response in a specific application.” [3] The host response, also known as biological response is the “observed reaction of a biological environment to a material.” [3] Because biocompatibility is not a material property, no material demonstrates biocompatibility in all applications. Thus, biocompatibility is evaluated from the biological or host response to the material for a specific function.

No biomaterial is perfectly inert or bioactive. An inert biomaterial is a material that does not actively react with the host biological environment. A bioactive biomaterial is a material that has an effect on the host biological system. Once implanted, biomaterials can generate different host responses. Host responses or biological responses can be acute or chronic. Clotting or inflammation, for example, could be an acute or chronic response depending on the duration and complexity of the reaction.

Despite the significant amount of research in this field, developing a completely non-thrombogenic material has proven to be a difficult task. [6] Tactics utilized in attempt to solve this drawback include surface treatments and coatings to improve the blood-compatibility of materials. [7] Although protein adsorption is the first step that occurs when protein is exposed to an artificial surface, the mechanisms behind this phenomenon are poorly understood. [2] However, it has been well established that contact activation initiates the coagulation cascade and ultimately leads to thrombus formation. In order to produce materials that are better tolerated by the body, more knowledge of the biological-surface interactions is necessary.

Material characterization is an important tool in analyzing surface properties. Determining the properties of the outermost layer of a material is essential because this is the surface that contacts the biological environment. The biological response to implanted biomaterials is affected by surface properties such as surface energy, chemistry and wettability; therefore, obtaining structure-property relationships that relate surface properties to thrombogenicity is ideal in order to obtain a material that resists thrombus formation. [6] There are several techniques available to determine different material properties. Unfortunately, one characterization method is not capable of providing all material surface properties. [5] Previous research has shown that varying water wettability of a surface has an affect on induced plasma coagulation time in-vitro. [6]

Contact angle analysis gives information on the wettability of a material and is advantageous to other characterization methods because it is a relatively low cost analysis. [5] Some contact angle methods include Wilhelmy plate method, capillary rise method and sessile drop method. [8] The wettability of a material can range from hydrophilic to hydrophobic. Figure 1 illustrates the contact angle measurements between a hydrophilic and hydrophobic surface and water.

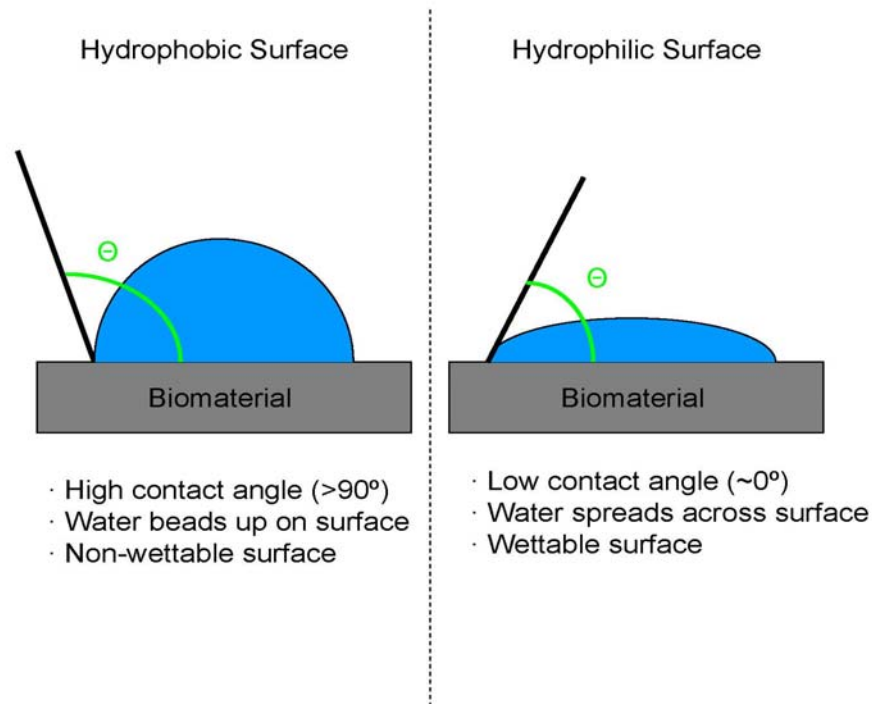


Figure 1: Illustration of contact angles on hydrophilic and hydrophobic surfaces

Contact angle analysis evaluates the capability of a liquid to spread on a surface. Water will expand to reach a force equilibrium when placed on a surface, in which the sum of the interfacial tensions is equal to zero, as shown in equation 1: [5]

$$\tau = \gamma_{sv} - \gamma_{ls} = \gamma_{lv} \cos \theta = 0 \quad [1]$$

where, τ is the adhesion tension, γ_{sv} is the solid-vapor surface tension, γ_{ls} is the liquid-solid surface tension and γ_{lv} is the liquid-vapor surface tension. The contact angle, θ , measures the ability of water to wet the surface. Smaller contact angles imply a hydrophilic surface, while larger contact angles suggest a hydrophobic surface. This phenomenon is due to the fact that water will spread to a greater extent on a hydrophilic surface and bead up on a hydrophobic surface. [5] An example of a hydrophobic material is poly (tetrafluoroethene), or PTFE. An example of a hydrophilic material is clean glass, which typically has a contact angle of approximately 0° . [6, 9]

In order to better study the interaction between hydrophilic and hydrophobic surfaces and their affect on blood coagulation, model procoagulant materials can be developed. Producing procoagulants with varying water wettability is an effective method to study and develop structure-property relationships between a material and the biological system.

1.3 Blood and Coagulation

Following the implantation of a biomaterial or device, blood will be the first fluid to contact the material's surface. [5] Blood is a circulating tissue whose primary function is to supply nutrients and remove waste products. [10] Whole blood consists of a fluid phase and a cellular phase. Plasma, the fluid phase of blood, represents 55% of blood volume, while other cellular elements comprise the remaining 45%. These cellular elements include red blood cells, also called erythrocytes, white blood cells, also called leukocytes and other cell fragments, known as platelets. Generally, plasma is a straw-yellow colored fluid; sometimes having a pink hue. Plasma consists of water, salts and plasma proteins. [10] The salts contained in plasma include sodium, potassium, calcium, magnesium, chloride and bicarbonate. [5] The plasma proteins present can be grouped into three different categories: albumin, globulins and clotting proteins. Particularly, the clotting proteins are involved in the coagulation cascade. Thus, plasma contains all essential proteins to support clot formation. Coagulated plasma forms a gelatinous mass or gel network. [6, 9] A variety of proteins play a role in the coagulation cascade, a table of these clotting factors and their properties are listed in appendix A. Upon initial discovery, the clotting factors involved in the cascade were assigned Roman numerals. The Roman numerals were designated in order of discovery, however at that time their role in the cascade was unknown. [11]

Clot formation proceeds through a number of zymogen-enzyme conversions; this sequence of events is known as the coagulation cascade, shown in figure 2. The intrinsic, extrinsic and common pathways are the three main pathways of the cascade. The cascade can be initiated by the intrinsic or extrinsic pathway. These two schemes eventually unite into the common pathway, where thrombin is generated. In return, thrombin reacts with

fibrinogen to form an insoluble fibrin clot or gel. Coagulation is a cascade of zymogen-enzyme conversions; therefore the enzyme or product of one reaction can activate other inactive molecules in the cascade. Thus, the complexity of this system and the succession of enzyme activation can quickly amplify into thrombus formation. [11]

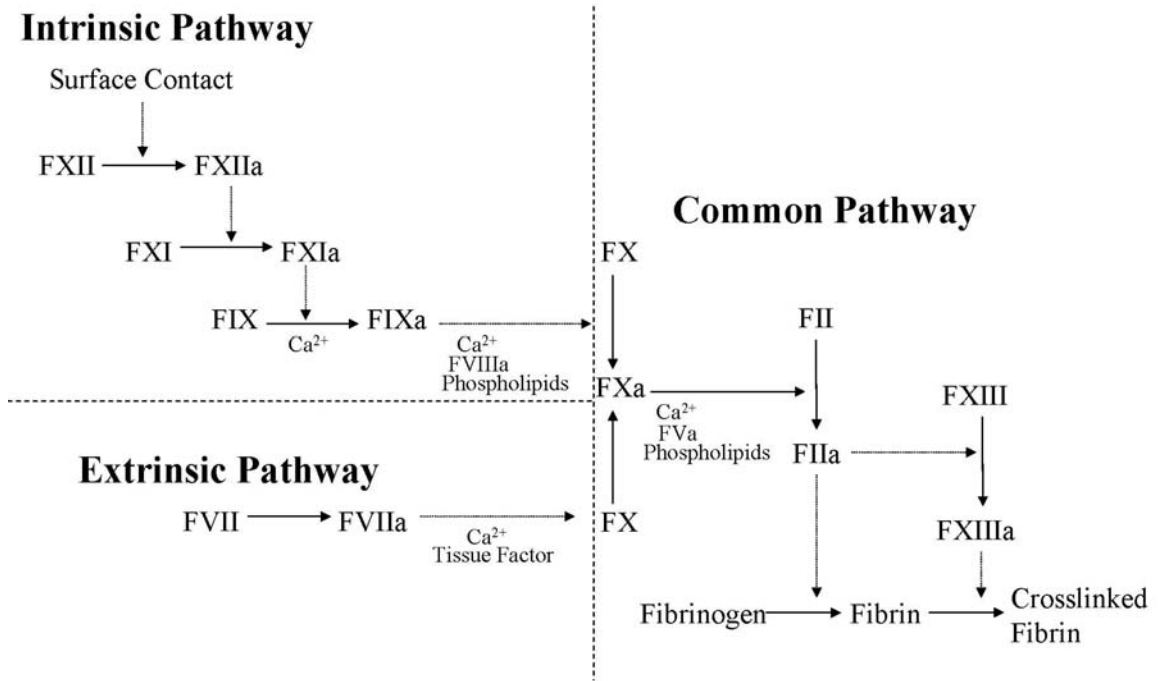


Figure 2: The Coagulation Cascade illustrating the three different pathways: intrinsic, extrinsic and common pathway. Source: Hanson, Stephen R. "Blood Coagulation and Blood-Materials Interactions." *Biomaterials Science: An Introduction to Materials in Medicine*. 2nd edition. Edited by B.D Ratner, AS Hoffman, Schoen FJ, JE Lemons. San Diego: Elsevier Academic Press, 2004. 332-345.

The common pathway of the cascade generates an enzyme called thrombin, also known as Factor IIa (FIIa). This is a key enzyme involved in the cascade because its interaction with fibrinogen forms fibrin, another principal enzyme in the cascade. Fibrin is the end product of the coagulation cascade. When thrombin acts upon its substrate fibrinogen, fibrin monomers are formed which oligomerize to form a gel. [11]

The extrinsic pathway of coagulation is initiated upon interaction between Factor VII (FVII) and tissue factor, a cell membrane protein. Tissue factor exists in human body tissues and is exposed upon vessel injury. [11] Therefore, this pathway is considered to be initiated in-vivo by disruption to a blood vessel. [11] Tissue factor interacts with Factor VII (FVII) and creates an activated enzyme, Factor VIIa (FVIIa). Subsequently, Factor X (FX) is activated and leads into the common pathway of the cascade.

The intrinsic pathway of coagulation commences by the activation of Factor XII (FXII) by a biomaterial surface, also called contact activation. All of the coagulation factors within the intrinsic pathway are present within plasma. Figure 3 portrays the contact activation mechanism. A procoagulant surface converts zymogen Factor XII (FXII) into Factor XIIa (FXIIa) and/or Factor XII_f (FXII_f); FXIIa in return activates Factor XI (FXI) to Factor XIa (FXIa) and prekallikrein to kallikrein. [11] The intrinsic pathway continues through these zymogen-enzyme conversions, ultimately forming Factor X (FX) which begins the common pathway of the cascade. Because of the importance of contact activation, more knowledge on this system will be useful in developing non-thrombogenic biomaterials or biomaterial interactions with blood.

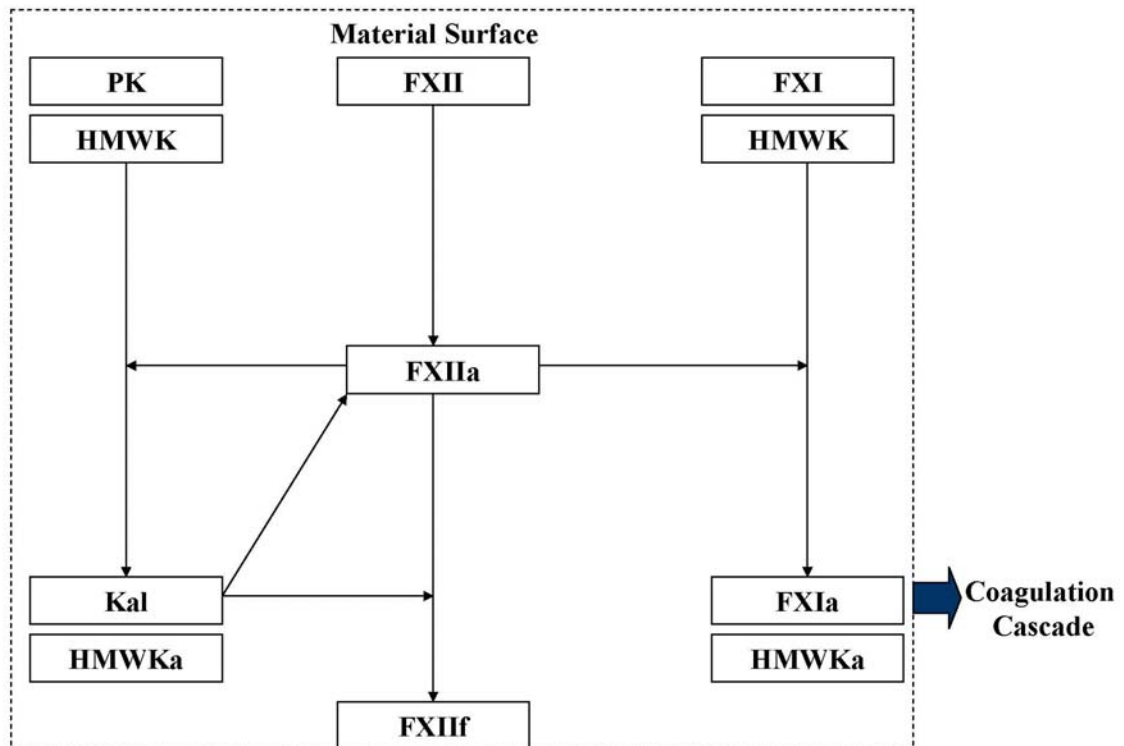


Figure 3: Contact activation of blood coagulation

1.4 Chromogenic Substrates

Enzymes are proteins that catalyze the chemical reactions that occur in the body. The substrate is the chemical compound acted upon by the enzyme. Enzymes react with chromogenic substrates forming color, shown by a spectrophotometer at 405 nm. [12] Chromogenic substrates are synthetically designed to function as the natural substrate. Chromogenic substrate technology was developed in the 1970's and has been deemed important in blood coagulation research. [12] Because of synthetic chromogenic substrate's ability to detect low amounts of protein, chromogenic substrates are useful in determining enzyme activity. [12] Chromogenic assays are an alternative to plasma coagulation assays that offer direct and specific detection of various factors such as FXIIa and FXIII [13].

1.5 Objectives

Understanding the bio-interactions upon initiation of the intrinsic coagulation cascade will provide useful information in order to better comprehend coagulation and the development of more hemocompatible biomaterials. Plasma coagulation time assays combined with chromogenic assays can detect and quantify surface activation. The aim of this study is seeking to:

- measure and compare clot times of FXIIa and FXII_f in solution that relate CT to [FXIIa] and [FXII_f]
- quantify enzyme activity of FXIIa and FXII_f in solution with chromogenic assay
- determine and compare amounts of FXIIa produced from solid procoagulants by plasma coagulation assay and chromogenic assay

Chapter 2. MATERIALS AND METHODS

2.1 Materials

2.2.1 General Materials

Water was obtained from Millipore water brand Simplicity ®185 water purification system to remove organic and inorganic contaminants with a total organic content (TOC) less than 5 ppb, less than 1 cfu/mL of micro-organisms and a resistivity of 18.2 MΩ-cm at 25 °C. [14] Chloroform and 2-propanol obtained from VWR were used to clean glassware prior to use.

Buffers required for use in assays were phosphate buffered saline (PBS, 140mM NaCl, 0.0027 M KCl, pH=7.4 at 25 °C, Sigma) dissolved into 1 L of water and Tris/HCl buffer (0.05 M Tris/HCl (Sigma), 0.012 M NaCl (Sigma), pH 7.8).

All assays were performed using outdated human plasma blood products anticoagulated with calcium chelator/preservative CPDA-1 (Citrate Phosphate Dextrose Adenine) from M.S. Hershey Medical Center Blood Bank. In-vitro plasma coagulation assays require 0.1 M calcium chloride (CaCl₂, Sigma), a recalcifying agent [6, 9], to allow the coagulation cascade to continue.

Coagulation assays performed in VWR 12 X 75 mm culture tubes were rinsed with Millipore water and dried before use. Additionally, Falcon and Becton Dickinson 15mL polypropylene tubes were rinsed with Millipore water and dried prior to use, for storage of human platelet poor plasma (PPP). Chromogenic assays were performed in VWR microcuvettes. Model procoagulants were prepared in VWR 15mm Pyrex glass petri dishes.

All weight measurements were made on a Mettler Toledo scale. Coagulation assays were performed on a Roto-Shake Genie (Scientific Industries, Inc.) hematology mixer at 8 rpm, to adequately mix the solution in the vials. Chromogenic assays were performed using a Beckman Coulter UV-VIS Spectrophotometer. Contact angle measurements were performed on Wilhelmy Balance equipment (Camtel, Ltd). All

glassware was cleaned prior to use with a glow-discharge Harrick Plasma Cleaner at 100 watts for at least 10 minutes.

2.1.2 Platelet Poor Plasma (PPP)

Human platelet poor plasma (PPP) was prepared from outdated (within two days of expiration) lots obtained from the M.S. Hershey Medical Center Blood Bank. This work was performed with a single lot of pooled plasma aliquoted into 15mL polypropylene tubes (Falcon, Becton Dickinson) and frozen at -20 °C until use. Consistent results are observed with plasma prepared and stored in this manner over about 1 year of experimentation. Experience has shown that different lots of plasma yield quantitatively different but qualitatively similar results. [6, 9]

2.1.3 Coagulation Proteins

Human coagulation FXII, FXIIa and FXIIa β (specified herein as FXII β) were obtained from Enzyme Research Laboratories (South Bend, IN) frozen in a 4mM sodium acetate-HCl/0.15 M NaCl buffer at pH 5.3. FXIIa activity was specified by the vendor in tradition units of PEU/mL. [15] FXII β was specified by the vendor in units of mg/mL but the absolute activity of the preparation was unknown. FXII was specified by the vendor in units of PEU/mL and mg/mL. Neat FXII, FXIIa and FXII β solutions were prepared in PBS.

2.1.4 Chromogenic Substrate

Chromogenic substrate s-2302 (H-D-Pro-Phe-Arg-pNA... 2HCl, MW=611.6 used as received from Diapharma Group Inc., Columbus, OH) structure is illustrated in figure 4.

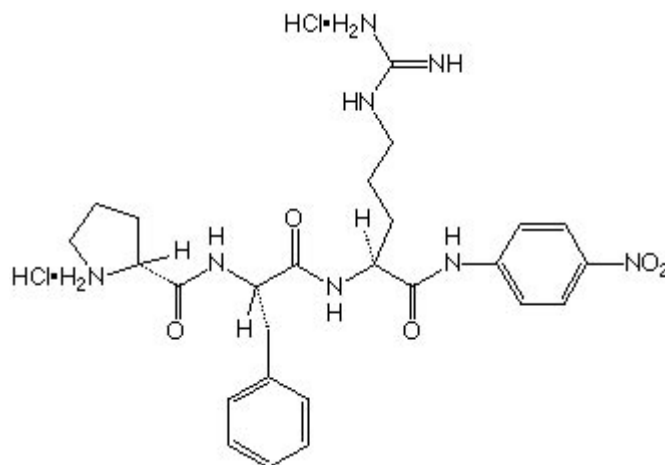


Figure 4: S-2302 Structure [12]

The 25 mg vial was used to prepare a 4.0 mM stock solution stored in 2-8 °C.

2.1.5 Procoagulant Surfaces

Test procoagulants applied in this work were 424-600 μm diameter glass beads (Sigma Aldrich) in either cleaned or silanized form. Each contact-activation experiment used 100 mg glass beads corresponding to approximately 500mm^2 surface area based on a nominal diameter of 500 μm . Clean-glass procoagulants were prepared in a 15mm Pyrex glass petri dish and 3 times serial rinses in 18 M Ω water, 2-propanol and chloroform. This was followed by air-plasma treatment of a single layer of washed-glass beads for ten minutes at 100 watts of plasma. Clean-glass beads were silanized by 1.5 h. reaction with 5% v/v OTS, Octadecyltrichlorosilane, (United Chemical Technologies, Inc.) in chloroform. Silanized beads were 3 times rinsed in chloroform and dried in a vacuum oven at 110 °C for 24 h. Contact angles of glass witness samples measured by Wilhelmy balance tensiometry (CDCA-100, Camtel Ltd.) yielded advancing $0^\circ/0^\circ$ and $110^\circ/83^\circ$ for clean and OTS-treated glass, respectively. Contact angle cannot be read directly on glass beads; therefore, 1.5-1.8 X 90 mm capillary tubes (Kimble Glass, Inc.) were used as glass witness samples. Optical microscopy of the shape of the liquid meniscus of beads partly immersed in water on a microscope slide qualitatively confirmed that the treated beads were not different from the witness samples. [6, 9]

In this study, test procoagulants prepared as above are referred to herein as “hydrophilic” (clean glass) or “hydrophobic” (silanized glass). In plasma coagulation in-vitro, coagulation time has been shown to scale sharply with different procoagulant properties energy leading to a contrast between surface types. [6, 9]

2.2 Methods

2.2.1 Plasma Coagulation Time Assay for FXIIa and FXIIb

The basic protocol for the coagulation time assay applied in this work has been described elsewhere [6, 9]. Plasma coagulation time (CT) was used as the traditional hematology method [9] to quantify FXIIa and FXIIb in solution through “FXIIa titration” and “FXIIb titration” calibration curves, respectively, that relate CT to [FXIIa] and [FXIIb]; where the square bracket denote concentrations expressed in PEU/mL or mg/mL for FXIIa and mg/mL for FXIIb. The protocol for this assay is depicted in figure 5. FXIIa and FXIIb titrations were carried out by equilibrating 0.5 mL of thawed plasma in polystyrene culture tubes and mixing with increasing volumes of FXIIa or FXIIb solution in PBS and diluting with sufficient additional PBS to bring the total volume to 900 μ L. Coagulation was induced by re-calcification with 100 μ L of 0.1 M CaCl_2 and contents were mixed on a slowly turning hematology mixer. CT after re-calcification was noted by a distinct change in fluid-like rheology to gel formation, allowing determination of the end point of the coagulation process to within 10 s or so [9]. CT was observed to be sensitive to FXIIa and FXIIb. FXIIa and FXIIb CT's yield a linear calibration curve on logarithmic [FXIIa] and [FXIIb] axes, respectively.

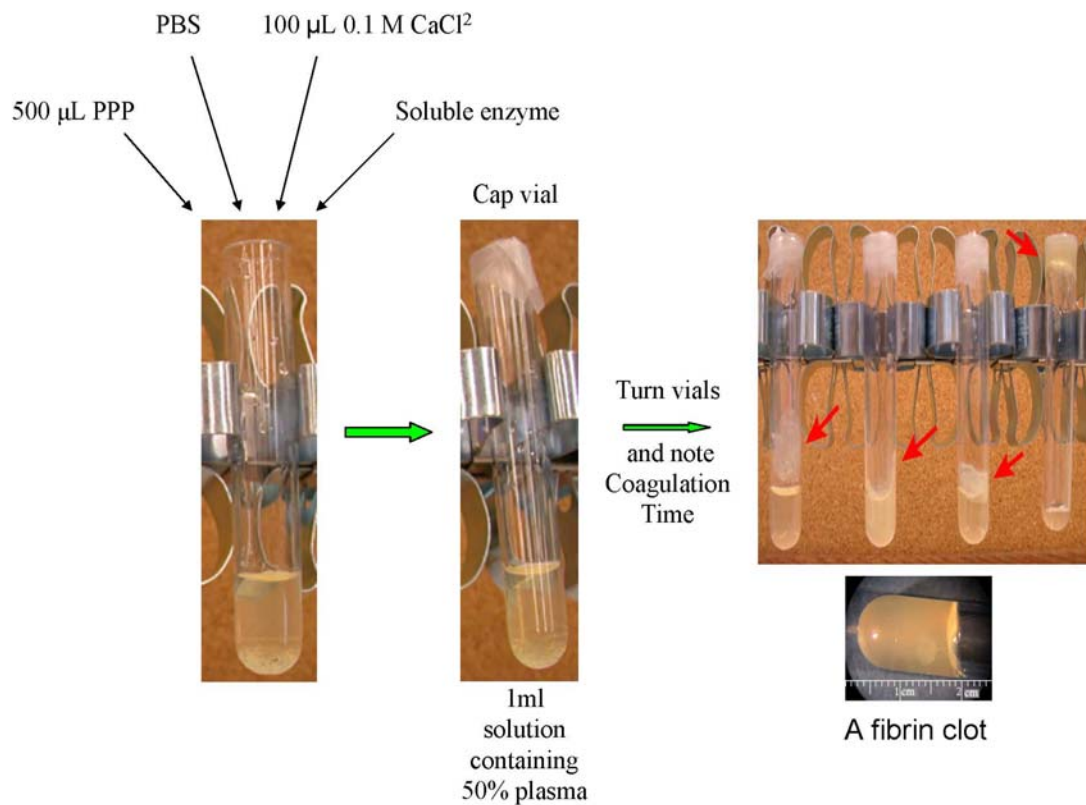


Figure 5: Schematic illustration of the in-vitro coagulation assay depicting reagents and materials used, procedure and end result. Pictures courtesy of Kaushik Chatterjee.

2.2.2 Chromogenic Assay for FXIIa and FXII_f

The basic experimental protocol for the chromogenic assay applied to this work has been described elsewhere [13]. Amidolytic activity of FXIIa and FXII_f was measured using a chromogenic substrate s-2302 (H-D-Pro-Phe-Arg-pNA... 2HCl, MW=611.6). The chromogenic assay was used to quantify FXIIa and FXII_f for comparison to plasma coagulation assays. A 4.0 mM stock solution of chromogen was prepared in 18 MΩ water and stored at 2-8 °C for no more than 6 months. A 0.4 mM working solution was prepared by diluting the stock solution 10-fold with buffer (0.05M Tris/HCl, 0.012 M NaCl pH 7.8). The actual FXIIa and FXII_f assay was performed by mixing 900 μL of working solution with 100 μL of test solution in a ultra-microcuvette (VWR) held in the chamber of an automatically recording UV-VIS spectrophotometer

(DU® Series 500, Beckman Coulter, Inc., Fullerton, CA). Absorbance change at 405 nm was recorded for 5 min to determine the initial velocity of color development. The calculated rate from these results was used to plot absorbance rate (in mAbs/min) by FXII concentration in terms of FXIIa and FXIIf concentration.

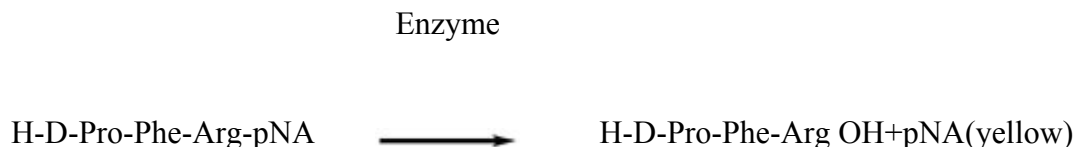


Figure 6: Principle of chromogenic substrates and color formation

The method to determine the activity of an enzyme is based on the difference in absorbance (optical quality), between the original substrate and the pNA formation or yellow color formation, as illustrated in figure 6. The slope is proportional to the enzymatic activity, determined by a spectrophotometer. [12]

2.2.3 Surface activation of FXII in neat-buffer solution

The basic experimental protocol for the surface activation method applied to this work has been described elsewhere [9]. The experimental strategy of FXII activation in neat-buffer solution (no proteins other than FXII and activation products therefrom) is illustrated in figure 7. Test solutions were purified FXII in PBS buffer at physiological concentration 30 µg/mL. [9] Putative FXIIa produced by contact with hydrophilic or hydrophobic procoagulant surfaces was either released into solution (free) or remained associated with activating surfaces (bound). Supernate containing free FXIIa was separated from surface-bound FXIIa by decantation, as shown in figure 7. Free FXIIa activity was quantified by measuring CT of PPP upon addition of supernate, with reference to the FXIIa titration curve. Additionally, free FXIIa activity was quantified by measuring the absorbance rate of the chromogenic substrate upon addition of supernate, with reference to the FXIIa titration curve.

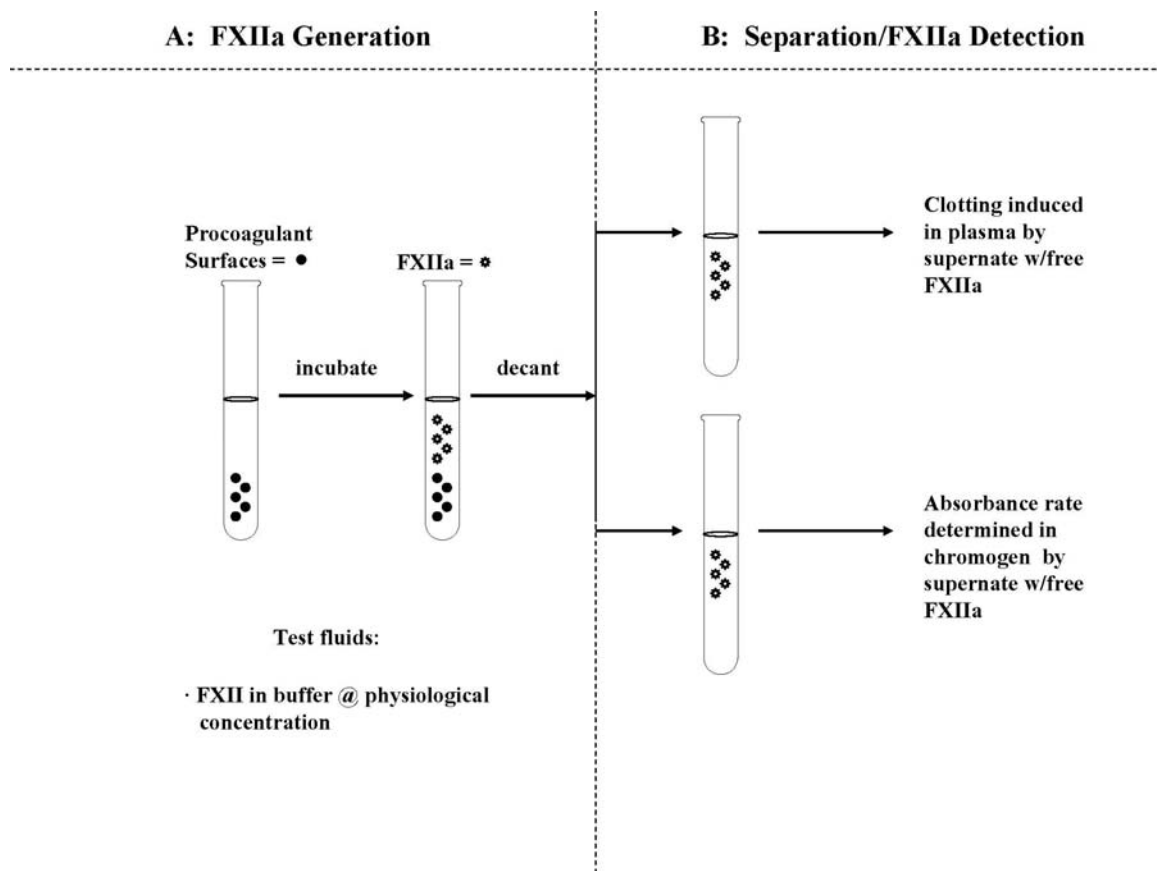


Figure 7: Experimental outline for detection of FXIIa produced by contact with procoagulant surfaces. A test solution of exogenous FXII at 30 $\mu\text{g}/\text{mL}$ with hydrophilic and hydrophobic surfaces produces putative FXIIa by contact for controlled time of $0 < t < 60$ minutes. After separation, presence of FXIIa was detected in plasma and chromogen by applying calibration curves obtained from plasma coagulation assays and chromogenic assays, respectively.

2.2.4 Statistical Analysis

Statistical analysis was performed using Sigma Plot version 10. In addition, propagation of error estimate was used to determine the error at each incubation time for contact activation experiments. The calculations for propagation of error estimates are included in appendix B.

Chapter 3. RESULTS

3.1 Plasma Coagulation Time Assay for FXIIa and FXIIb

FXIIa is a vital enzyme involved in the coagulation cascade. Exogenous FXIIa and FXIIb were used as controls to measure and compare CTs of plasma. The plasma coagulation assay quantifies FXIIa and FXIIb in solution through “FXIIa titration” and “FXIIb titration” respectively. Titration curves were produced by protocol explained in section 2.1. The FXIIa titration is shown in figure 8. The FXIIa calibration curve on log-normal coordinates is shown in figure 9.

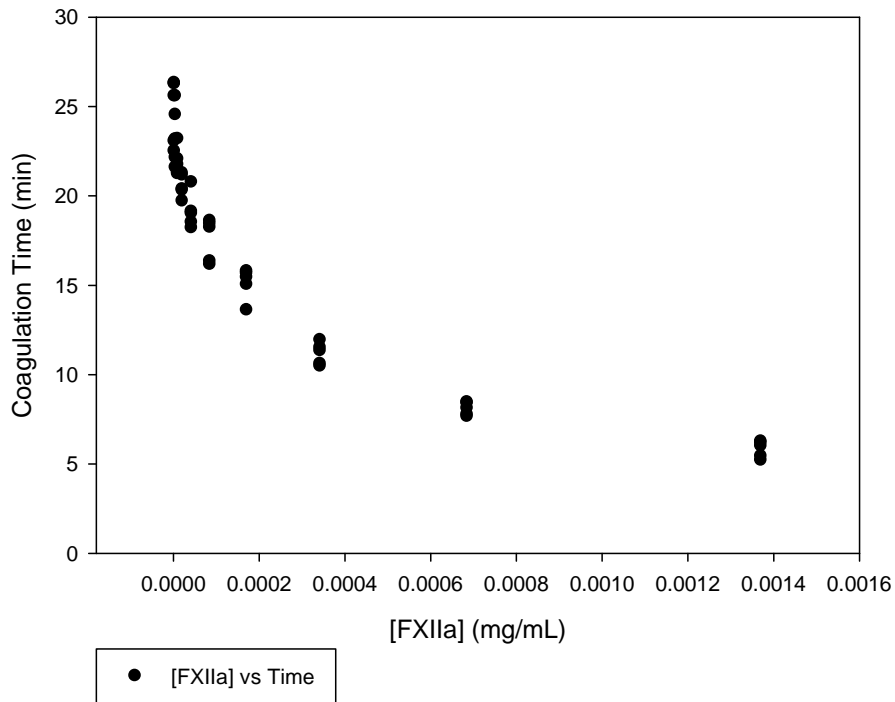


Figure 8: FXIIa titration of PPP that relates observed plasma coagulation time to FXIIa concentration where $n=5$.

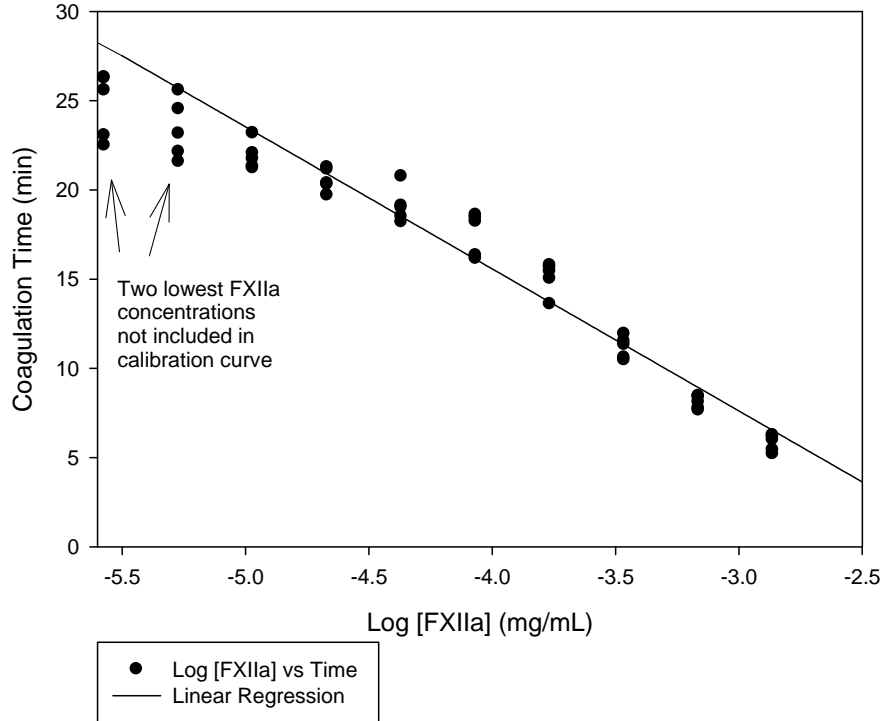


Figure 9: FXIIa calibration curve obtained through exogenous FXIIa titration on log concentration axis where $n=5$. The line drawn through the data is a result of linear-least-squares regression through the interval 1.07×10^{-5} mg/mL to 1.37×10^{-3} mg/mL FXIIa concentration; ($CT = (-7.9 \pm 0.3) \log[FXIIa] - 16.3 \pm 1.1$, $R^2 = 95.3\%$).

Figure 8 relates CT to [FXIIa]; where the square brackets indicate concentrations in mg/mL. Results plotted on log-normal coordinates, as shown in figure 9, show a linear calibration curve. In order to obtain a precise calibration curve, the two lowest FXIIa concentrations, 5.35×10^{-6} mg/mL and 2.67×10^{-6} mg/mL, were not included in the linear-least-squares regression. This reveals a practical calibration curve with FXIIa concentration ranging from 1.07×10^{-5} mg/mL to 1.37×10^{-3} mg/mL with good linearity:

$$CT = (-7.9 \pm 0.3) \log[FXIIa] - 16.3 \pm 1.1, R^2 = 95.3\%$$

This linear equation follows the form $y = m \log[FXIIa] + b$

The slope of this equation has the units (min · mL)/mg. In order to compare results from FXIIa and FXIIc calibration curves on a weight and molar basis, this slope is converted in terms of (min · mL)/mol. A comparison by molar basis is important for these two

enzymes because of the differences in their molecular weights. The slope of the FXIIa calibration curve is $-7.9 \text{ (min} \cdot \text{mL)/mg}$ or $-6.4 \times 10^8 \text{ (min} \cdot \text{mL)/mol}$.

The role of FXII_f in the coagulation cascade is investigated to determine if it has procoagulant activity. Additionally, as stated earlier, comparison between the FXIIa coagulation assay and FXII_f coagulation assay is necessary. The FXII_f titration is shown in figure 10. The FXII_f calibration curve on log-normal coordinates is shown in figure 11.

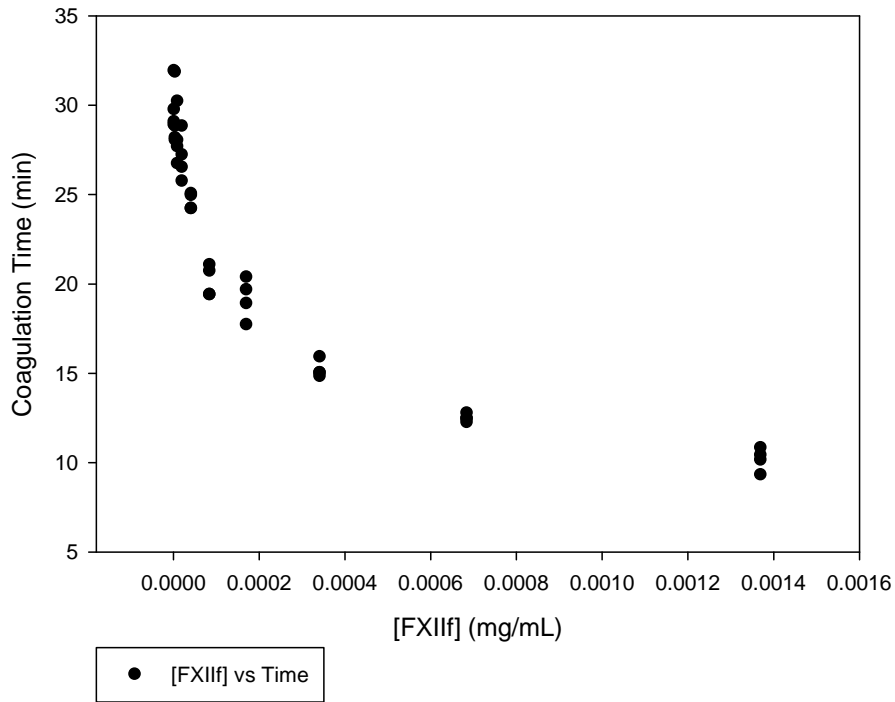


Figure 10: FXII_f titration of PPP that relates observed plasma coagulation time to FXII_f concentration where n=4.

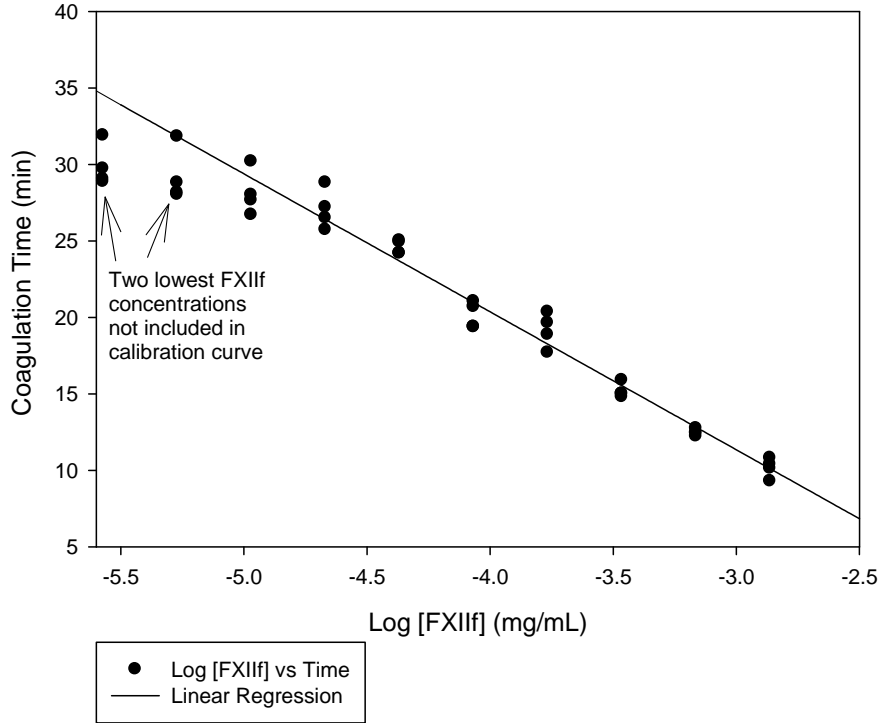


Figure 11: FXIIIf calibration curve obtained through exogenous FXIIIf titration on log concentration axis where $n=4$. The line drawn through the data is a result of linear-least-squares regression through the interval 1.07×10^{-5} mg/mL to 1.37×10^{-3} mg/mL FXIIIf concentration; $(CT = (-9.0 \pm 0.3) \log[FXIIIf] - 15.7 \pm 1.1, R^2 = 97.1\%)$.

Figure 10 relates CT to [FXIIIf]; where the square brackets indicate concentrations in mg/mL. Results plotted on log-normal coordinates, as shown in figure 11, show a linear calibration curve. In order to obtain a precise calibration curve, the two lowest FXIIIf concentrations, 5.35×10^{-6} mg/mL and 2.67×10^{-6} mg/mL, were not included in the least-linear-squares regression. This reveals a practical calibration curve with FXIIIf concentration ranging from 1.07×10^{-5} mg/mL to 1.37×10^{-3} mg/mL with good linearity:

$$CT = (-9.0 \pm 0.3) \log[FXIIIf] - 15.7 \pm 1.1, R^2 = 97.1\%$$

This linear equation follows the form $y = m \log[FXIIIf] + b$

The slope of this equation has the units (min · mL)/mg. As stated earlier, this slope is converted in terms of (min · mL)/mol for comparison to the FXIIa calibration curve. The slope of the FXIIIf calibration curve is -9.0 (min · mL)/mg or -2.5×10^8 (min · mL)/mol.

3.2 Contact angle measurements of procoagulant materials

Figures 12 and 13 show the Force (mN) versus Immersion Depth (mm) of hydrophilic procoagulants and hydrophobic procoagulants, respectively. Using the Young equation, equation 1, and implementing force calculations for the Wilhelmy plate method obtains receding and advancing contact angles. Hydrophobic procoagulants yielded a receding contact angle of 83° and an advancing contact angle of 110° . Hydrophilic procoagulants yielded a receding and advancing contact angle of 0° . Contact angle calculations can be found in appendix B.

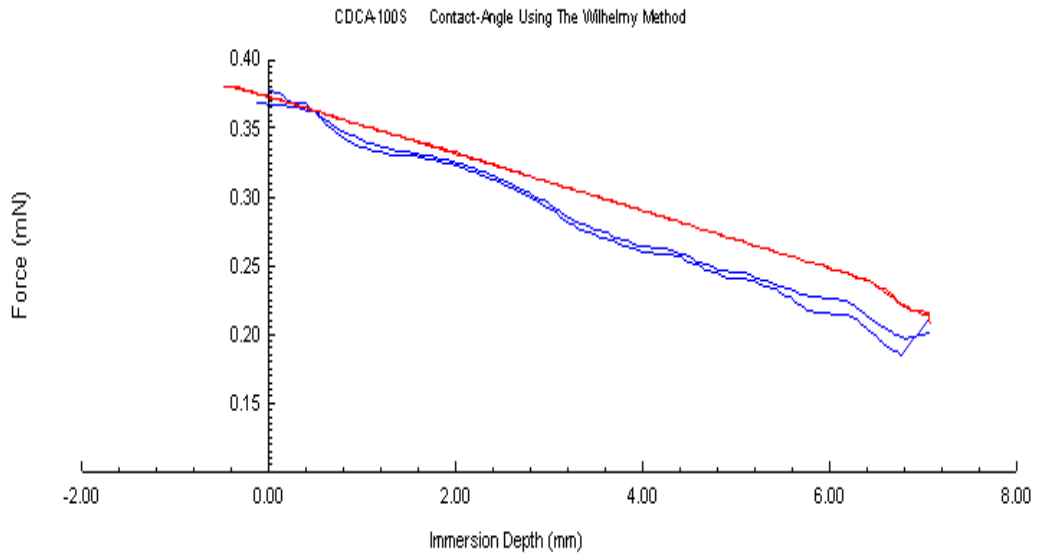


Figure 12: Plot of Force (mN) vs. Immersion Depth (mm) of hydrophilic procoagulants using the wilhelmy method.

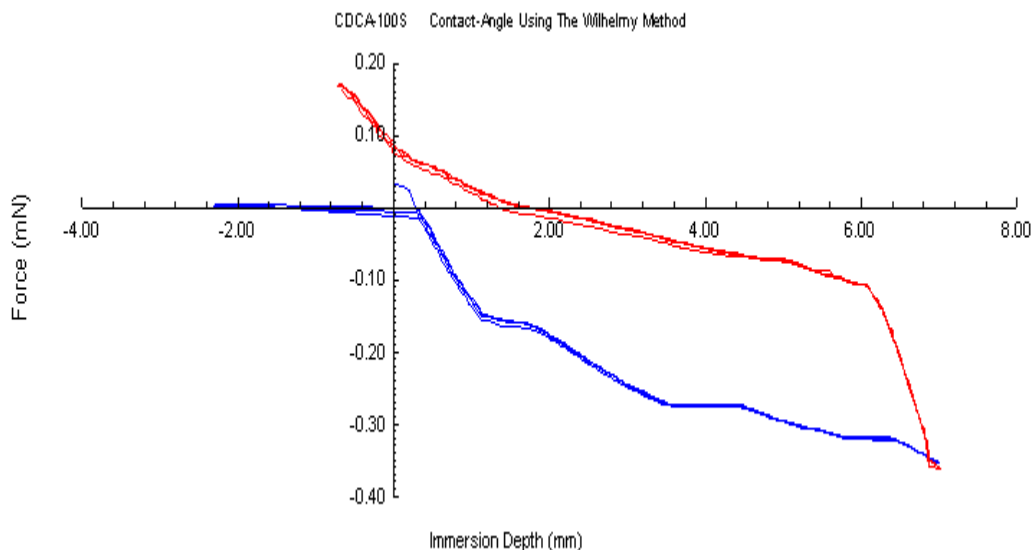


Figure 13: Plot of Force (mN) vs. Immersion Depth (mm) of hydrophobic procoagulants using the Wilhelmy method.

3.3 FXIIa generation by surface activation of FXII in neat buffer solution by plasma coagulation assay

Figure 14 illustrates how responsive plasma coagulation was to various measures of exogenous FXIIa (shown in Section 3.1) and is utilized herein as a calibration curve to determine amounts of putative FXIIa by surface activation. In order to obtain and compare amounts of putative FXIIa produced by surface activation in plasma and chromogen, FXIIa concentration was measured in PEU/mL for both experiments. This being said, the calibration curve plots FXIIa concentration in PEU/mL; opposed to the original FXIIa calibration curve with FXIIa concentration plotted in mg/mL. Plotting results on log-normal coordinates provide a linear calibration curve; omitting the lowest FXIIa concentrations, 1.95×10^{-4} PEU/mL and 3.90×10^{-4} PEU/mL reveals a practical calibration curve with FXIIa concentration ranging from 7.81×10^{-4} PEU/mL to 0.1 PEU/mL with good linearity:

$$CT = (-7.9 \pm 0.3) \log[\text{FXIIa}] - 1.4 \pm 0.6, R^2 = 95.3\%$$

This linear equation follows the form $y = m \log[\text{FXIIa}] + b$

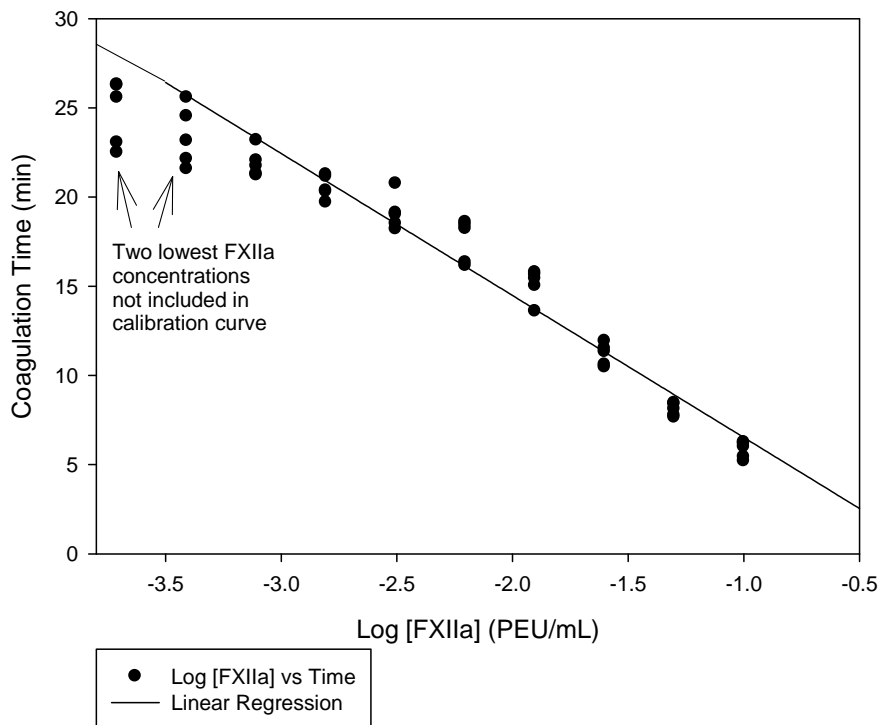


Figure 14: FXIIa calibration curve obtained through exogenous FXIIa titration on log concentration axis. The line drawn through the data is a result of linear-least-squares regression through the interval 7.81×10^{-4} PEU/mL to 0.1 PEU/mL FXIIa concentration; $(CT = (-7.9 \pm 0.3) \log[FXIIa] - 1.4 \pm 0.6, R^2 = 95.3\%)$.

Data collected in table 1 compiles results of contact activation experiments by quantifying putative FXIIa generated in FXII neat buffer solution (by utilizing the FXIIa calibration curve of figure 14). Figure 15 compares kinetics of free FXIIa generated by contact with hydrophilic and hydrophobic procoagulants in neat buffer solution. FXIIa activation was instantaneous in both hydrophilic and hydrophobic procoagulants; shown by a mean value of FXIIa generation drawn as a straight line through the data. FXIIa yield at hydrophobic procoagulants was 2-fold higher than at hydrophilic procoagulants.

Table 1. Contact activation of FXII neat buffer solution induced by contact with hydrophilic (clean glass) and hydrophobic (silanized glass) bead procoagulants producing FXIIa by plasma coagulation assay. Each incubation experiment used 100 mg of glass beads corresponding to approximately 500 mm² surface area based on a nominal diameter of 500 μm. FXII solution prepared in PBS at a concentration of 30 μg/mL.

Incubation Time (min.)	Procoagulant Surface (500 mm²) Type	Supernate FXIIa/mL (PEU X 10⁻²)
	Hydrophilic	
1		0.64 ± 0.16
5		0.55 ± 0.14
10		0.76 ± 0.19
15		0.84 ± 0.20
20		0.83 ± 0.20
25		0.82 ± 0.20
30		0.80 ± 0.19
60		0.85 ± 0.21
	Hydrophobic	
1		1.43 ± 0.33
5		1.99 ± 0.45
10		1.76 ± 0.18
15		2.34 ± 0.52
20		1.88 ± 0.43
25		1.83 ± 0.41
30		1.75 ± 0.40
60		1.42 ± 0.33

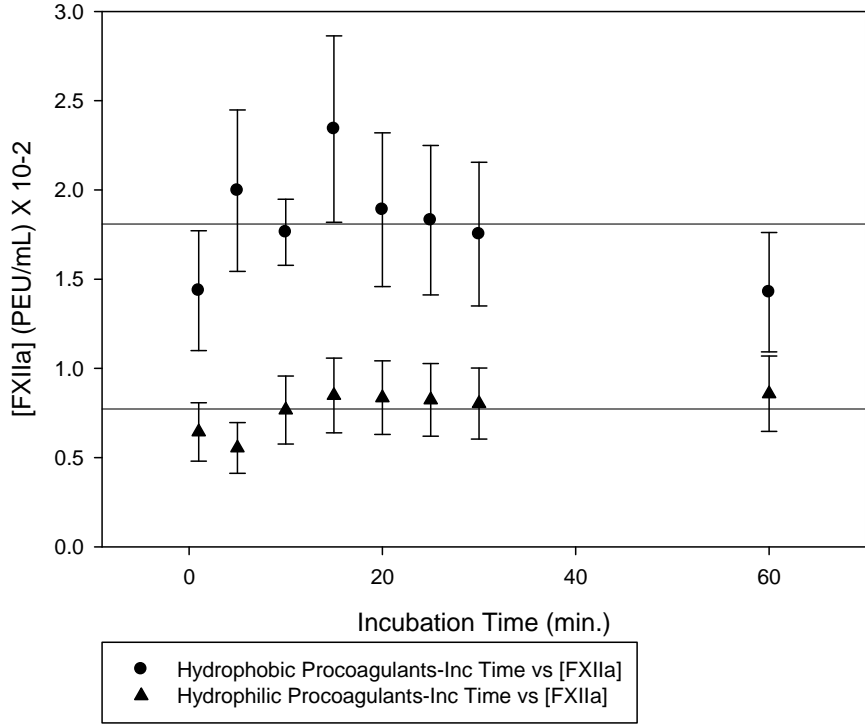


Figure 15: FXIIa generation in neat FXII solution at 30 $\mu\text{g/mL}$ induced by contact with 500 mm^2 surface area of hydrophobic and hydrophilic procoagulants. Lines drawn through the data are the mean value of FXIIa generation.

3.4 Chromogenic Assay for FXIIa and FXII_f

Because color development is dependent upon FXII concentration [15], plotting absorbance rate versus FXIIa concentration in terms of varying FXII concentrations, as shown in figure 16, gives a reliable chromogenic assay. The absorbance rate is calculated from the slope of color formation against time at 405 nm for each [FXIIa] dissolved in serially increasing concentrations of FXII. Absorbance rates at varying [FXII] were found to systematically increase to a maximum rate V_{\max} at swamping [FXII] greater than 30 $\mu\text{g/mL}$. Therefore, autohydrolysis is a significant reaction with the FXIIa chromogenic assay. [13]

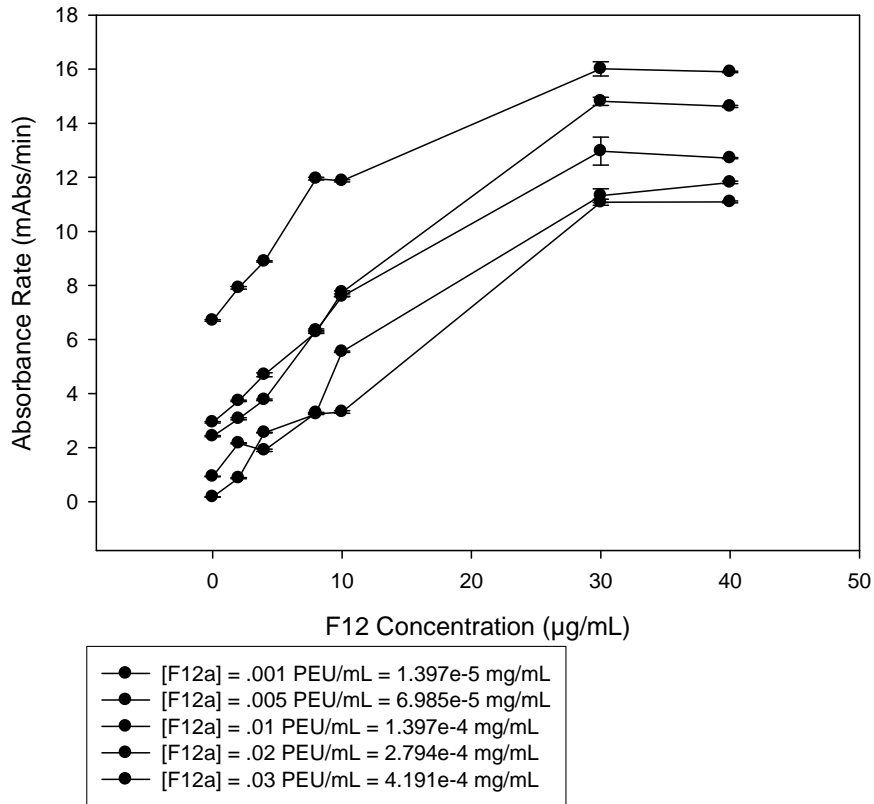


Figure 16: Color development kinetics for chromogenic FXIIa assay performed in neat-buffer solutions of FXII. Absorbance rate ($\Delta A/\text{min}$) was measured and calculated at 5 min. Lines are drawn through the data to guide the eye. Notice that rate ($\Delta A/\text{min}$) is a strong function of FXII concentration.

A linear correlation between V_{\max} and [F12a] was observed, as shown in figure 17 and 18, where figure 17 displays the different absorbance rates obtained from using two different lots of enzyme. This would reveal two different calibration curves; lot 1 serves as a rate-assay calibration curve over the range $0.001 \text{ PEU/mL} < [\text{FXIIa}] < 0.03 \text{ PEU/mL}$ while lot 2 serves as a rate-assay calibration curve over the range $0.04 \text{ PEU/mL} < [\text{FXIIa}] < 0.09 \text{ PEU/mL}$. This reveals two rate-assay calibration curves:

$$\text{Lot 1: } \Delta A/\text{min} = (168.9 \pm 7.5)[\text{FXIIa}] + 11.0 \pm 0.1; R^2=99.4\%$$

$$\text{Lot 2: } \Delta A/\text{min} = (110.4 \pm 6.6)[\text{FXIIa}] + 10.1 \pm 0.4; R^2=98.6\%$$

Both of these linear equations follow the form $y = m[\text{FXIIa}] + b$

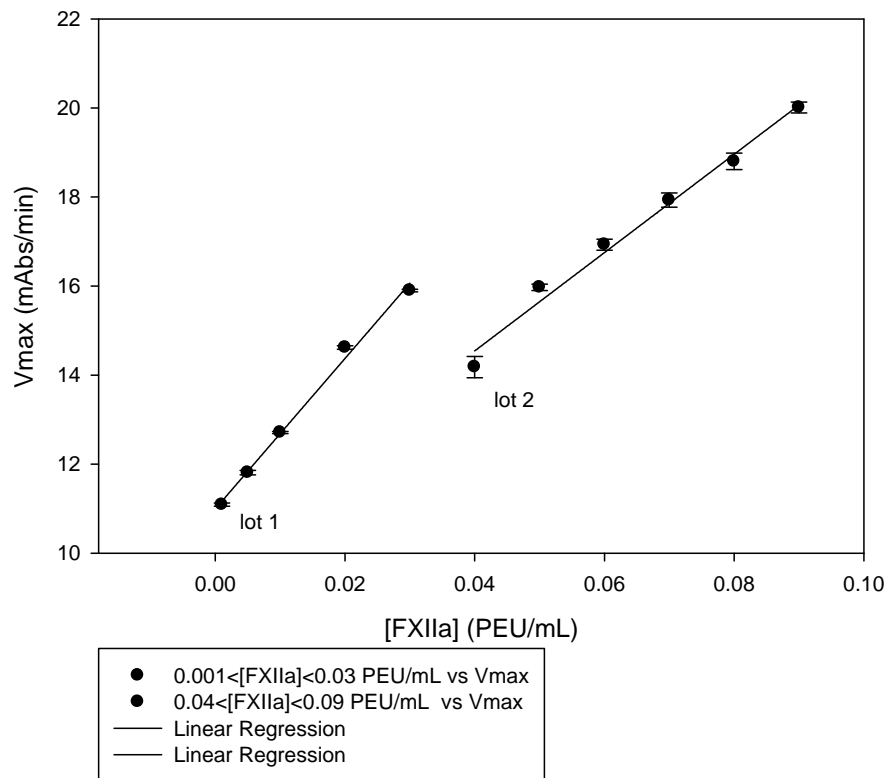


Figure 17: Linear correlation between V_{\max} (measured in $40 \mu\text{g/mL}$ solution) and [FXIIa]. The line drawn through lot 1 data is a result of linear-least squares regression revealing $\Delta A/\text{min} = (168.9 \pm 7.5)[\text{FXIIa}] + 11.0 \pm 0.1; R^2=99.4\%$). The line drawn through lot 2 data is a result of linear-least squares regression revealing $\Delta A/\text{min} = (110.4 \pm 6.6)[\text{FXIIa}] + 10.1 \pm 0.4; R^2=98.6\%$.

Although two different lots of enzyme were used, combining these two lots into 1 rate-assay calibration curve is shown in figure 18. This reveals a rate-assay calibration curve over the range $0.001 < [\text{FXIIa}] < 0.09 \text{ PEU/mL}$:

$$\Delta A/\text{min} = (89.7 \pm 7.9)[\text{FXIIa}] + 11.7 \pm 0.4; R^2=93.3\%$$

This linear equation follows the form $y = m[\text{FXIIa}] + b$

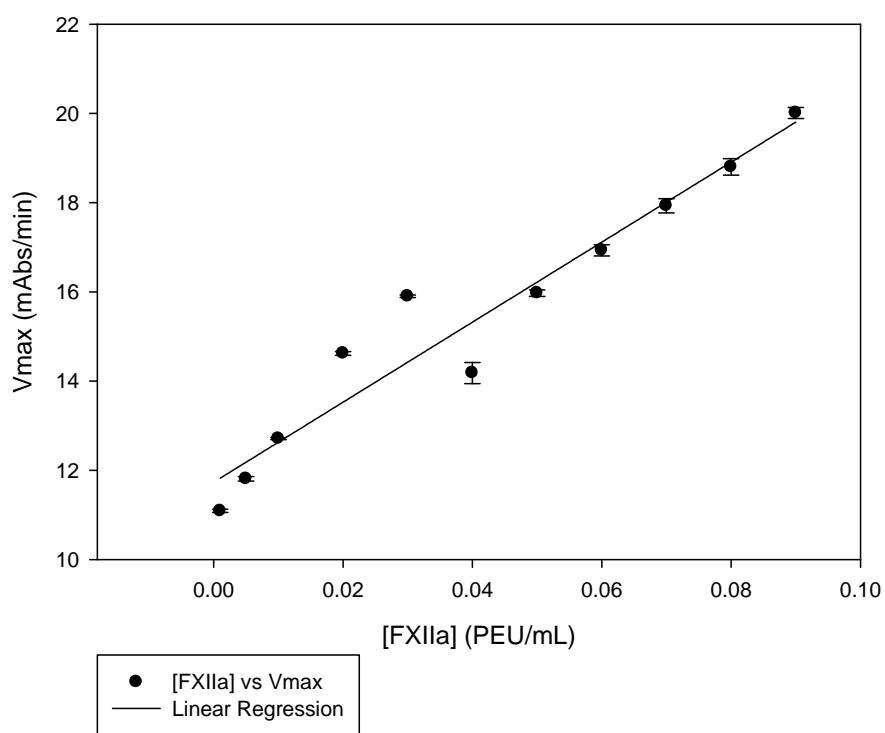


Figure 18: Linear correlation between V_{\max} (measured in $40 \mu\text{g/mL}$ solution) and $[\text{FXIIa}]$. The line drawn through the data is a result of linear-least squares regression revealing $\Delta A/\text{min} = (89.7 \pm 7.9)[\text{FXIIa}] + 11.7 \pm 0.4; R^2=93.3\%$.

Although the two different lots of enzyme produced different outcomes, combining results into one rate-assay calibration curve still shows good linearity with a R^2 of 93.3%. However, a smaller slope is attributed to the rate-assay calibration curve when results are combined. A larger slope is acquired from the rate-assay calibration curves when results are not combined. Nonetheless, autohydrolysis is a significant reaction with the FXIIa chromogenic assay, shown figures 16, 17 and 18. [13]

To determine if FXII_f had amidolytic activity, a FXII_f chromogenic assay was developed. Absorbance rate versus FXII_f concentration in terms of varying FXII concentrations is shown in figure 19. The absorbance rate is calculated from the slope of color formation against time at 405 nm for each [FXII_f] dissolved in serially increasing concentrations of FXII. Absorbance rates at varying [FXII] were found to slightly increase; however, unlike the FXII_a chromogenic assay, there is a slight apparent FXII effect on color development. Therefore, autohydrolysis is not as significant of a reaction in FXII_f chromogenic assay as in the FXII_a chromogenic assay.

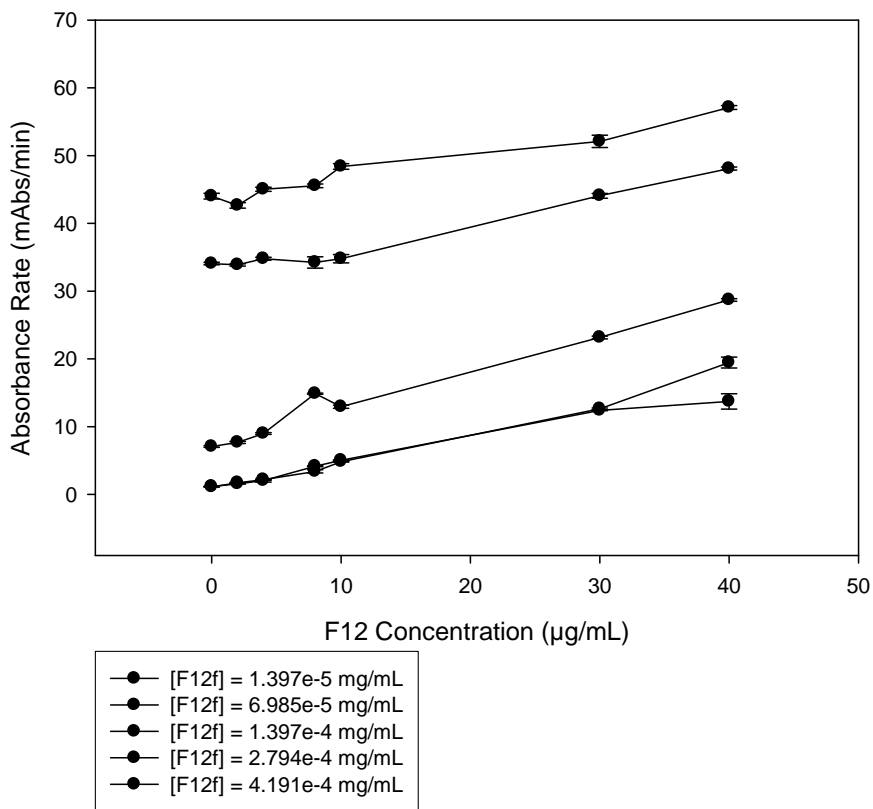


Figure 19: Color development kinetics for chromogenic FXII_f assay performed in neat-buffer solutions of FXII. Absorbance rate ($\Delta A/\text{min}$) was measured and calculated at 5 min. Lines are drawn through the data to guide the eye. Notice that rate ($\Delta A/\text{min}$) is not a strong function of FXII concentration.

3.5 FXIIa generation by surface activation of FXII in neat buffer solution by chromogenic assay

Figure 20 illustrates how responsive chromogen was to various measures of exogenous FXIIa and is utilized herein as a calibration curve to determine amounts of putative FXIIa by surface activation. A practical calibration curve with FXIIa concentration ranging from 3.12×10^{-3} PEU/mL to 0.1 PEU/mL with good linearity:

$$\Delta A/\text{min} = (11.8 \pm 0.6) [\text{FXIIa}] + 0.4 \pm 0.03, R^2 = 98.6\%$$

This linear equation follows the form $y = m[\text{FXIIa}] + b$

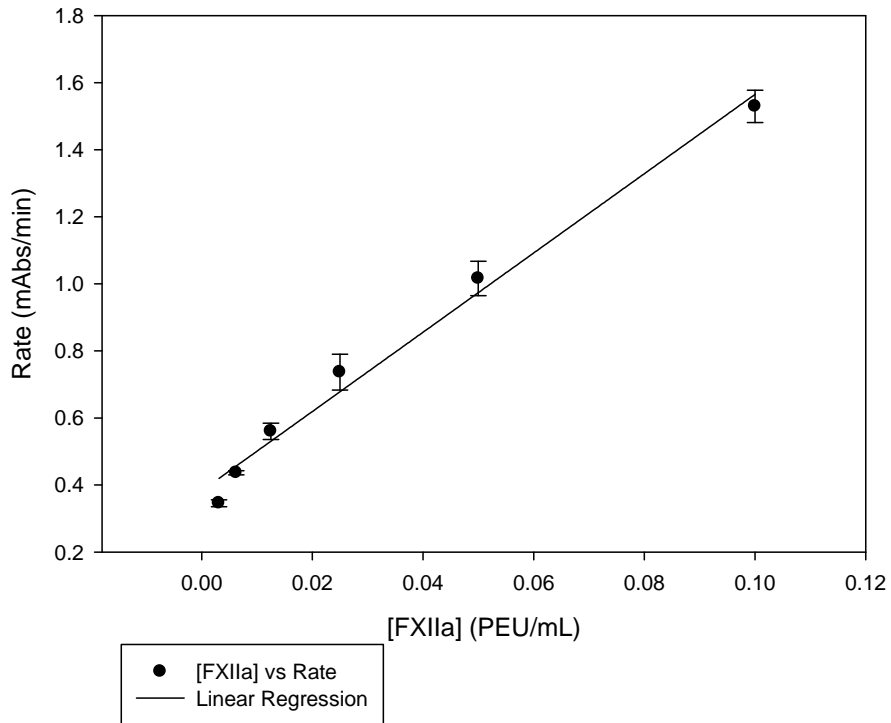


Figure 20: FXIIa calibration curve that relates absorbance rate ($\Delta A/\text{min}$) to FXIIa concentration obtained through exogenous FXIIa titration of chromogenic substrate. Absorbance rate was measured and calculated at 5 min. The line drawn through the data is a result of linear-least-squares regression through the interval shown; ($\Delta A/\text{min} = (11.8 \pm 0.6) [\text{FXIIa}] + 0.4 \pm 0.03, R^2 = 98.6\%$).

Data collected in table 2 compiles results of contact activation experiments by quantifying putative FXIIa generated in FXII neat buffer solution (by utilizing the FXIIa calibration curve of figure 20). Figure 21 compares kinetics of free FXIIa generated by contact with hydrophilic and hydrophobic procoagulants in neat buffer solution. FXIIa activation was instantaneous; shown by a mean value of FXIIa generation drawn as a straight line through the data. FXIIa yield at hydrophobic procoagulants was higher than at hydrophilic procoagulants.

Table 2. Contact activation of FXII neat buffer solution induced by contact with hydrophilic (clean glass) and hydrophobic (silanized glass) bead procoagulants producing FXIIa by chromogenic assay. Each incubation experiment used 100 mg of glass beads corresponding to approximately 500 mm² surface area based on a nominal diameter of 500 µm. FXII solution prepared in PBS at a concentration of 30 µg/mL.

Incubation Time (min.)	Procoagulant Surface Type (500 mm²)	Supernate FXIIa/mL (PEU X 10⁻²)
	Hydrophilic	
1		0.63 ± 0.27
5		1.22 ± 0.28
10		0.77 ± 0.28
15		1.02 ± 0.28
20		0.68 ± 0.27
25		0.88 ± 0.28
30		1.30 ± 0.28
60		0.45 ± 0.27
	Hydrophobic	
1		6.22 ± 0.45
5		6.94 ± 0.49
10		7.32 ± 0.51
15		6.63 ± 0.47
20		5.19 ± 0.41
25		5.28 ± 0.41
30		5.86 ± 0.44
60		5.60 ± 0.42

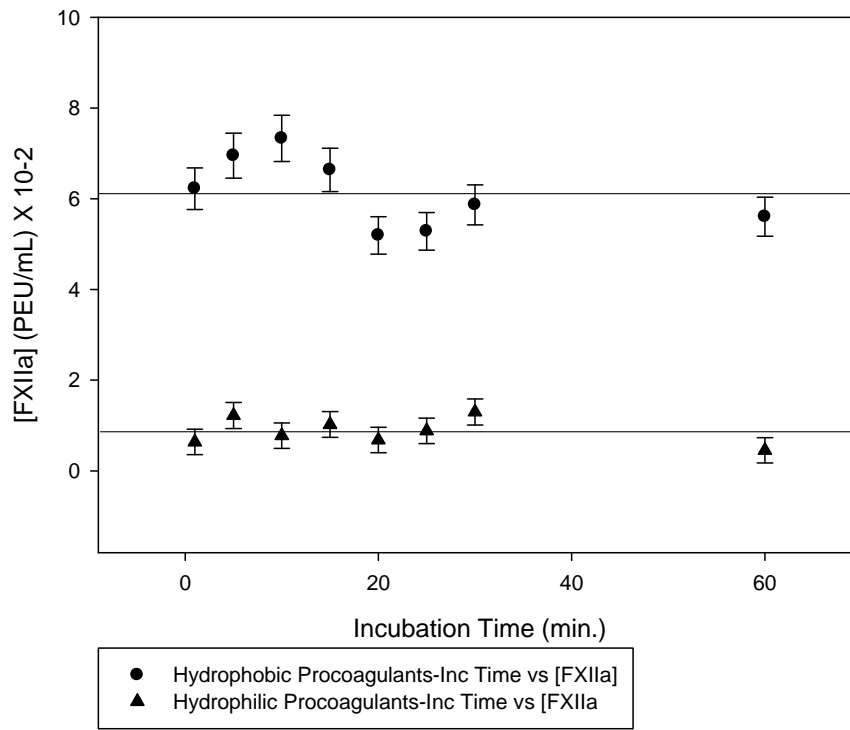


Figure 21: FXIIa generation in neat FXII solution at 30 $\mu\text{g/mL}$ induced by contact with 500 mm^2 surface area of hydrophobic and hydrophilic procoagulants. Lines drawn through the data are the mean value of FXIIa generation.

Chapter 4. DISCUSSION

4.1 Plasma Coagulation Time Assay for FXIIa and FXIIf

Used as a traditional hematology method [9], plasma coagulation assays are readily used for the detection of enzymatic activity and in-vitro surface activation of the coagulation cascade. FXIIa and FXIIf titration curves in plasma, shown in figure 8, 9, 10 and 11, verify that plasma is a sensitive assay for both enzymes. Additionally, the obtained log dose-response curves for both enzymes in plasma seem to parallel each other. Similar empirical trends were obtained for the equivalent doses of enzyme and both curves didn't account for the two lowest concentrations achieving a more precise curve. However, data shows that longer CTs were obtained with FXIIf than FXIIa in plasma. Furthermore, the slope of the FXIIf log-normal calibration curve appears to be steeper than the FXIIa log-normal calibration curve. But, since both enzymes have different molecular weights, the slopes of FXIIa and FXIIf log-normal calibration curves were converted to molar basis for a better comparison. Results on a molar basis show that FXIIa is 2.6 times stronger procoagulant than FXIIf. Taken together, these results show that FXIIa and FXIIf both have procoagulant activity and play a major role in the CTs of plasma. Hence, more information on the contact activation mechanism, specifically quantifying FXIIa and FXIIf production and the factors influencing this generation is essential.

4.2 FXIIa generation by surface activation of FXII in neat buffer solution by plasma coagulation assay

Data collected in table 1 displays a quantitative comparison of FXIIa generation produced by the interaction of hydrophilic and hydrophobic procoagulants with FXII neat buffer solution. Likewise, figure 15 graphs the kinetics of putative FXIIa generation. Lines drawn through the data are an average of concentrations produced therefore FXIIa generation was instantaneous with hydrophilic procoagulants. However, FXII → FXIIa with hydrophobic procoagulants appears almost instantaneous, requiring nearly 5 minutes for an apparent conversion. Or, this reduction of FXIIa at the 1 minute incubation period could be due to autoinhibition. Additionally, reduced generation of FXIIa at 60 minute

incubation period with hydrophobic procoagulant could be due to autoinhibition.

Autoinhibition is a feedback loop that inhibits FXIIa actions; however it is unclear if this phenomenon is implied from these studies.

Previous work by R. Zhuo et al demonstrated that hydrophobic procoagulants contact with FXII neat buffer solution produced more putative FXIIa than hydrophilic procoagulants. [9] Specifically, hydrophobic procoagulants appeared to generate FXIIa concentration 2-fold higher than hydrophilic procoagulants. Results from this work conclude the same effect. Yet, results from this work obtained FXIIa generation 2-fold lower for both hydrophilic and hydrophobic procoagulants. The reason for this inconsistency is unclear; however these differences could be attributed to the different coagulation factors and plasma lots used. Further investigation and analysis is desired to determine the relationship between surface-induced coagulation by procoagulant materials and FXIIa and FXIIf generation

4.3 Chromogenic Assay for FXIIa and FXIIf

For comparison of results in plasma to chromogen, a chromogenic assay was used to detect enzymatic activity and surface activation of the coagulation cascade. R. Zhuo et al previously established a FXIIa chromogenic assay, accounting for the autohydrolysis reaction by performing the FXIIa assay in swamping concentrations of FXII. [13] The results from this work show an analogous outcome. Figure 16 confirms autohydrolysis of FXII is a significant reaction in neat buffer solution containing FXII and FXIIa.

Additionally, FXIIa is apparently saturated with substrate and proceeds at maximum velocity V_{max} , when $[FXII] \geq 30 \mu\text{g/mL}$. A plot of $[FXIIa]$ versus V_{max} (when $[FXII] = 40 \mu\text{g/mL}$) confirms autohydrolysis is a significant reaction in neat buffer solutions and validates the reasoning behind accounting for this reaction. It is uncertain if autohydrolysis occurs in plasma, therefore more research on this phenomenon is necessary. Nonetheless, if autohydrolysis is a significant reaction in plasma, the reaction would also proceed at V_{max} because FXIIa concentrations would saturate with FXII at physiological concentrations. [13]

The practical FXIIa assay protocol was used to create a FXIIf chromogenic assay. Figure 19 reveals that autohydrolysis is not as noteworthy with the FXIIf chromogenic assay. Additionally, compared to the FXIIa assay, the FXIIf assay has a higher absorbance rate.

4.4 FXIIa generation by surface activation of FXII in neat buffer solution by chromogenic assay

Data collected in table 2 displays a quantitative comparison of FXIIa generation produced by interaction of hydrophilic and hydrophobic procoagulants with FXII neat buffer solution. Likewise, figure 21 graphs the kinetics of putative FXIIa generation. Lines drawn through the data are an average of concentrations produced therefore FXIIa generation was instantaneous with hydrophilic and hydrophobic procoagulants. However, there was greater error and a wider range of FXIIa concentrations obtained with hydrophobic procoagulants than hydrophilic procoagulants. The reason for a wider range of FXIIa concentrations with hydrophilic procoagulants could be due to autoinhibition. However, as stated earlier, it is unclear if this phenomenon is implied from these studies.

Hydrophobic procoagulants appeared to generate FXIIa concentration extensively higher than hydrophilic procoagulants. Therefore, FXIIa generation by incubation with FXII neat buffer solution with hydrophilic and hydrophobic procoagulants in chromogen and plasma produce similar results. Both experiments performed in chromogen and plasma show hydrophobic procoagulants generate more FXIIa than hydrophilic procoagulants. Hydrophilic procoagulants generate comparable amounts of FXIIa from plasma and chromogen. However, hydrophobic procoagulants do not generate comparable amounts of FXIIa from plasma and chromogen. In plasma, the average FXIIa generation is 1.80×10^{-2} PEU/mL. In chromogen, the average FXIIa generation is 6.13×10^{-2} PEU/mL. The reason for this inconsistency is unclear; however some differences could be attributed to the different coagulation factors lots used. However, the major difference could be due to the distinctive events that can occur in plasma verse chromogen.

Chapter 5. CONCLUSIONS

An in-vitro plasma coagulation assay was utilized to develop and compare dose-response curves for FXIIa and FXII_f. An alternative to the in-vitro coagulation assay is the chromogenic assay, which was utilized for detection of FXIIa and FXII_f as well. Additionally, model procoagulants in contact with FXII neat buffer solution generated putative FXIIa, used in both the plasma coagulation assay and chromogenic assay to determine the relationship between water wettability and FXIIa generation. These studies were performed aiming to gain more insight on the mechanisms involved in the contact activation of blood with a biomaterial surface.

Overall, assessment and analysis of the plasma coagulation cascade were made by plasma coagulation assays, chromogenic assays and contact activation experiments. Plasma coagulation assays demonstrate greater CTs with FXII_f than FXIIa, although the FXII_f calibration curve yields a steeper slope than FXIIa on a weight basis. However, FXIIa is 2.6 times stronger procoagulant than FXII_f on a molar basis. Utilizing chromogen and obtaining a FXIIa and FXII_f chromogenic assay illustrate that swamping concentrations of FXII lead to a V_{max} for FXIIa but not for FXII_f. The FXII_f chromogenic assay had less dependence on FXII concentration than the FXIIa chromogenic assay, in which the FXIIa assay results showed presence of autohydrolysis. More FXIIa was generated by hydrophobic procoagulants than hydrophilic procoagulants by surface activation of FXII in neat buffer solution by plasma coagulation assay and chromogenic assay. Some results herein show the possibility of an auto-inhibition reaction. However, from this study it is unclear whether this putative reaction is in fact occurring. More information about autohydrolysis, autoinhibition, the role of FXII_f in the coagulation cascade and the mechanisms behind the contact activation mechanism and how surface properties affect the propensity of this activation is essential to solve this biomedical challenge.

Evidently, additional investigation of the coagulation cascade and the components controlling contact activation is essential. Specific details regarding this phenomenon

will suggest methods to improve biomaterial blood-compatibility for cardiovascular applications. Suggestions for future work include:

1. Determine if autohydrolysis is a significant reaction in plasma by performing a plasma coagulation assay with FXII and FXIIa in buffer solution and compare to results from FXIIa plasma coagulation assay.
2. Perform gel electrophoresis experiments in combination with contact activation experiments in order to better determine the enzymes present upon FXII activation
3. Determine if auto-inhibition is a relevant reaction
4. Design experiments to acquire more knowledge concerning the role of FXII in contact activation since it is clear that the enzyme has amidolytic and plasma coagulation activity

BIBLIOGRAPHY

- [1] Heart Disease and Stroke Statistics [Brochure]. (2007) Dallas, TX: American Heart Association
- [2] Chandy T, Das GS, Rao Gundu HR, Wilson RF. "Use of plasma glow for surface-engineering biomolecules to enhance bloodbiocompatibility of Dacron and PTFE vascular prosthesis." *Biomaterials* 21 (2000) 699-712.
- [3] Hoffman AS, Lemons JE, Ratner BD, Schoen FJ. "Biomaterials Science: A Multidisciplinary Endeavor." Biomaterials Science: An Introduction to Materials in Medicine. 2nd edition. Edited by B.D Ratner, AS Hoffman, Schoen FJ, JE Lemons. San Diego: Elsevier Academic Press, 2004. 1-9.
- [4] Williams, DF. Definitions in Biomaterials. Proceedings of a Consensus Conference of the European Society for Biomaterials. Vol 4. New York: Elsevier 1986
- [5] Bizios R, Dee KC, Puleo DA. *Tissue-Biomaterial Interactions*. New Jersey: John Wiley & Sons, Inc., 2002
- [6] Bussard KM, Miller R, Siedlecki CA, Vogler EA, Zhuo R. "Procoagulant stimulus processing by the intrinsic pathway of blood plasma coagulation." *Biomaterials* 26 (2005) 2965-2973.
- [7] Guo Z, Miller R, Siedlecki CA, Vogler EA. "Plasma coagulation response to surfaces with nanoscale chemical heterogeneity." *Biomaterials* 27 (2006) 208-215.
- [8] Rater BD. "Surface Properties and Surface Characterization of Materials" Biomaterials Science: An Introduction to Materials in Medicine. 2nd edition. Edited by B.D Ratner, AS Hoffman, Schoen FJ, JE Lemons. San Diego: Elsevier Academic Press, 2004. 40-59.
- [9] Siedlecki CA, Vogler EA, Zhuo R. "Autoactivation of blood factor XII and hydrophilic and hydrophobic surfaces." *Biomaterials* 27 (2006) 4325-4332.
- [10] Malchesky, Paul S. "Extracorporeal Artificial Organs" Biomaterials Science: An Introduction to Materials in Medicine. 2nd edition. Edited by B.D Ratner, AS Hoffman, Schoen FJ, JE Lemons. San Diego: Elsevier Academic Press, 2004. 514-526.

- [11] Hanson, Stephen R. "Blood Coagulation and Blood-Materials Interactions." Biomaterials Science: An Introduction to Materials in Medicine. 2nd edition. Edited by B.D Ratner, AS Hoffman, Schoen FJ, JE Lemons. San Diego: Elsevier Academic Press, 2004. 332-345.
- [12] Chromogenic Substrates: Purified Proteins and Enzymes [Brochure]. (2004) DiaPharma Group, Inc.
- [13] Vogler EA, Zhuo R. "Practical application of a chromogenic FXIIa assay." *Biomaterials* 27 (2006) 4840-4845.
- [14] Simplicity Water Purification Systems [Brochure]. (2005) Billerica, MA: Millipore Corporation
- [15] Enzyme Research Laboratory Cascade [Brochure]. (2004) Enzyme Research Laboratories
- [16] Bach R, Konigsberg W, Nemerson Y. "Purification and Characterization of Bovine Tissue Factor." *Journal of Biological Chemistry* 256 (1981) 8324-8331.
- [17] Bouma BN, Cochrane CG, Griffin JH, Revak SD. "Surface and fluid phase activities of two forms of activated Hageman factor produced during contact activation of plasma." *Journal of Experimental Medicine* 147 (1978) 719-729.

APPENDICES

A. Coagulation Cascade Components

B. Calculations

APPENDIX A. Coagulation Cascade Components

Properties of clotting factors

Coagulation Factor Name	Common Name	Molecular Weight (Daltons)	Approximate Physiological Concentration (µg/mL)	Pathway in Coagulation Cascade
I	Fibrinogen	340,000 [11]	2500 [11]	Common [11]
II	Prothrombin	72,000 [11]	140 [11]	Common [11]
III	Tissue Factor, Thromboplastin	53,000[16]	---	Extrinsic [16]
V	Proaccelerin	330,000 [11]	5-12 [11]	Common [11]
VI	Unassigned	---	---	---
VII	Proconvertin	50,000 [11]	1 [11]	Extrinsic [11]
VIII	Antihemophilic Factor (AHF)	330,000 [11]	.2 [11]	Intrinsic [11]
IX	Partial Thromboplastin Component	57,000 [11]	3-5 [11]	Intrinsic [11]
X	Stuart-Power	59,000 [11]	5 [11]	Common [11]

	Factor			
XI	Plasma Thromboplastin Antecedent	143,000 [11]	3-6 [11]	Intrinsic [11]
XII	Hageman Factor	80,000 [11]	30 [11]	Intrinsic [11]
XIIa	---	80,000 [17]	*	Intrinsic []
XII_f	Factor FXII Fragments	28,000 [17]	*	Intrinsic []
XIII	Fibrin-Stabilizing Factor	320,000 [11]	10 [11]	Common [11]
Human Prekallikrein	Fletcher Factor	100,000 [11]	50 [11]	Intrinsic [11]
High Molecular Weight Kininogen	Fitzgerald Factor	120,000 [11]	80 [11]	Intrinsic [11]

* Depends on degree of activation in blood

APPENDIX B. Calculations

Propagation of error calculations

Propagation of error estimates were necessary for contact activation experiments to find the error attributed to each FXIIa concentration determined. Contact activation experiments performed in plasma and chromogen required different calculations based on the equation form of the calibration curve. Contact activation experiments performed in plasma obtained a linear calibration curve in the form of: $y = m \log [\text{FXIIa}] + b$. While contact activation experiments performed in chromogen obtained a linear calibration curve in the form of: $y = m [\text{FXIIa}] + b$. The propagation of error estimates how σ propagates into the calculated x values ([FXIIa]).

Propagation of error estimate:

$$\sigma^2 = \left(\frac{\partial y}{\partial m}\right)^2 \sigma_m^2 + \left(\frac{\partial y}{\partial b}\right)^2 \sigma_b^2 + \left(\frac{\partial y}{\partial x}\right)^2 \sigma_x^2 + \left(\frac{\partial y}{\partial n}\right)^2 \sigma_n^2$$

$$\sigma_y = \sqrt{\sigma_y^2}$$

Error calculations for contact activation experiments performed in plasma:

$$CT = m \log[\text{FXIIa}] + b$$

$$\left(\frac{CT - b}{m}\right) = \log[\text{FXIIa}]$$

$$[\text{FXIIa}] = 10^{\left(\frac{CT-b}{m}\right)} \equiv 10^y \text{ where, } y = \left(\frac{CT-b}{m}\right)$$

$$\sigma_{[\text{FXIIa}]}^2 = \left(\frac{\partial 10^y}{\partial m}\right)^2 \sigma_m^2 + \left(\frac{\partial 10^y}{\partial b}\right)^2 \sigma_b^2$$

$$\frac{\partial 10^y}{\partial m} = 10^y \ln 10 \frac{\partial y}{\partial m}$$

$$\frac{\delta 10^y}{\delta m} = 10^{\left(\frac{CT-b}{m}\right)} \ln 10 \frac{\delta \left(\frac{CT-b}{m}\right)}{\delta m}$$

$$\frac{\delta \left(\frac{CT-b}{m}\right)}{\delta m} = \frac{m(0) - (CT-b)(1)}{m^2}$$

$$\frac{\delta \left(\frac{CT-b}{m}\right)}{\delta m} = \frac{b - CT}{m^2}$$

$$\left(\frac{\delta 10^y}{\delta m}\right)^2 = \left[10^{\left(\frac{CT-b}{m}\right)} \ln 10 \left(\frac{b - CT}{m^2}\right)\right]^2$$

$$\left(\frac{\delta 10^y}{\delta m}\right)^2 = \left[2.303 \cdot 10^{\left(\frac{CT-b}{m}\right)} \cdot \left(\frac{b - CT}{m^2}\right)\right]^2$$

$$\frac{\delta 10^y}{\delta b} = 10^y \ln 10 \frac{\delta y}{\delta b}$$

$$\frac{\delta 10^y}{\delta b} = 10^{\left(\frac{CT-b}{m}\right)} \ln 10 \frac{\delta \left(\frac{CT-b}{m}\right)}{\delta b}$$

$$\frac{\delta \left(\frac{CT-b}{m}\right)}{\delta b} = \frac{m(-1) - (CT-b)(0)}{m^2}$$

$$\frac{\delta \left(\frac{CT-b}{m}\right)}{\delta b} = -\frac{1}{m}$$

$$\left(\frac{\delta 10^y}{\delta b}\right)^2 = \left[10^{\left(\frac{CT-b}{m}\right)} \cdot \frac{\ln 10}{-m}\right]^2$$

$$\left(\frac{\delta 10^y}{\delta b}\right)^2 = \left[\frac{2.303}{-m} \cdot 10^{\left(\frac{CT-b}{m}\right)}\right]^2$$

$$\sigma_{[y \text{ in } m]}^2 = \left[2.303 \cdot 10^{\left(\frac{CT-b}{m}\right)} \cdot \left(\frac{b - CT}{m^2}\right)\right]^2 \sigma_m^2 + \left[\frac{2.303}{-m} \cdot 10^{\left(\frac{CT-b}{m}\right)}\right]^2 \sigma_b^2$$

where $\sigma_m^2 = .2844^2$, $\sigma_b^2 = .6161^2$, $b = -1.438$, $m = -7.959$

Coagulation Time (CT)	Error (σ)
13.23	4.7409e-6
12.09	7.7993e-6
15.52	1.6843e-6
11.54	9.8677e-6
12.28	7.1850e-6
12.39	6.8505e-6
12.54	6.4180e-6
13.25	4.6992e-6
16.00	1.3491e-6
16.52	1.0590e-6
15.40	1.7800e-6
15.05	2.0898e-6
15.10	2.0426e-6
15.15	1.9964e-6
15.24	1.9157e-6
15.01	2.1284e-6

Error calculations for contact activation experiments performed in chromogen:

$y = m[\text{FXIIa}] + b$ where y = absorbance rate

$$[\text{FXIIa}] = \frac{y - b}{m}$$

$$\sigma_{[\text{FXIIa}]}^2 = \left(\frac{\delta \left(\frac{y - b}{m} \right)}{\delta m} \right)^2 \sigma_m^2 + \left(\frac{\delta \left(\frac{y - b}{m} \right)}{\delta b} \right)^2 \sigma_b^2$$

$$\left(\frac{\delta \left(\frac{y - b}{m} \right)}{\delta m} \right) = \frac{m(0) - (y - b)1}{m^2}$$

$$\left(\frac{\delta \left(\frac{y - b}{m} \right)}{\delta m} \right)^2 = \left(\frac{b - y}{m^2} \right)^2$$

$$\left(\frac{\delta \left(\frac{y - b}{m} \right)}{\delta m} \right) = \frac{m(-1) - (y - b)0}{m^2}$$

$$\left(\frac{\delta \left(\frac{y - b}{m} \right)}{\delta m} \right)^2 = \left(\frac{-1}{m} \right)^2$$

$$\sigma_{[\text{FXIIa}]}^2 = \left(\frac{b - y}{m^2} \right)^2 \sigma_m^2 + \left(\frac{-1}{m} \right)^2 \sigma_b^2$$

where $\sigma_m^2 = .6938^2$, $\sigma_b^2 = .03270^2$, $b = .3827$, $m = 11.82$

Y (Absorbance Rate)	Error (σ)
1.1180	4.5811e-3
1.2040	4.9283e-3
1.2490	5.1147e-3
1.1670	4.7773e-3
0.9964	4.1160e-3
1.007	4.1551e-3
1.076	4.4167e-3
1.0450	4.2977e-3
0.4582	2.7918e-3
0.5273	2.8582e-3
0.4745	2.8038e-3
0.5036	2.8309e-3
0.4636	2.7955e-3
0.4873	2.8148e-3
0.5364	2.8699e-3
0.4364	2.7793e-3

Contact angle calculations

Contact angle analysis was performed on hydrophilic and hydrophobic procoagulants. The receding and advancing contact angles, θ_r and θ_a , were calculated to confirm the wettability of the procoagulant glass beads prepared.

$$F = p \cdot \gamma_{lv} \cos \theta$$

$$\text{where } p = 2\pi r, r = .0015, \gamma_{lv} = 71.97 \text{ @ } T (^{\circ}\text{C}) = 25^{\circ}\text{C}$$

For hydrophilic procoagulants:

$$F_r = .37 \text{ obtained from graph of Force (mN) verse Immersion Depth (mm)}$$

$$\theta_r = 0^{\circ}$$

$$F_a = .34 \text{ obtained from graph of Force (mN) verse Immersion Depth (mm)}$$

$$\theta_a = 0^{\circ}$$

For hydrophobic procoagulants:

$$F_r = .04 \text{ obtained from graph of Force (mN) verse Immersion Depth (mm)}$$

$$\theta_r = 83^{\circ}$$

$$F_a = -.12 \text{ obtained from graph of Force (mN) verse Immersion Depth (mm)}$$

$$\theta_a = 110^{\circ}$$